Published in final edited form as:
Physiol Genomics. 2006 April 13; 25(2): 263–276.

High-Throughput Identification of IMCD Proteins Using LC-MS/MS

Trairak Pisitkun[1], **Jared Bieniek**[1], **Dmitry Tchapyjnikov**[1], **Guanghui Wang**[2], **Wells W. Wu**[2], **Rong-Fong Shen**[2], and **Mark A. Knepper**[1]

1 *Laboratory of Kidney and Electrolyte Metabolism, National Heart, Lung, and Blood Institutes, National Institutes of Health, Bethesda, MD 20892, USA*

2 *Proteomics Core Facility, National Heart, Lung, and Blood Institutes, National Institutes of Health, Bethesda, MD 20892, USA*

Abstract

The inner medullary collecting duct (IMCD) is an important site of vasopressin-regulated water and urea transport. Here we have used protein mass spectrometry to investigate the proteome of the IMCD cell, and how it is altered in response to long-term vasopressin administration in rats. IMCDs were isolated from inner medullas of rats, and IMCD proteins were identified by liquid chromatography/tandem mass spectrometry (LC-MS/MS). We present a WWW-based "IMCD Proteome Database", containing all IMCD proteins identified in this study (n = 704) and prior MS-based identification studies (n = 301). We used the isotope-coded affinity tag (ICAT) technique to identify IMCD proteins that change in abundance in response to vasopressin. dDAVP or vehicle was infused subcutaneously in Brattleboro rats for 3 days and IMCDs were isolated for proteomic analysis. dDAVP and control samples were labeled with different cleavable ICAT reagents (mass difference 9 amu) and mixed. This was followed by 1-D SDS-PAGE separation, in-gel trypsin digestion, biotin-avidin affinity purification, and LC-MS/MS identification and quantification. Responses to vasopressin for a total of 165 proteins were quantified. Quantification based on semiquantitative immunoblotting of 16 proteins for which antibodies were available showed a high degree of correlation with ICAT results. In addition to aquaporin-2 and γ -ENaC, five of the immunoblotted proteins were substantially altered in abundance in response to dDAVP, viz. syntaxin-7, Rap1, GAPDH, HSP70, and cathepsin D. A 28-protein vasopressin signaling network was constructed using literature-based network analysis software focusing on the newly identified proteins, providing several new hypotheses for future studies.

Index words

systems biology; mass spectrometry; aquaporin-2; ENaC; vasopressin

Introduction

Vasopressin controls renal water excretion in part by regulating the permeability of collecting duct cells to water. The main protein target for this process is the water channel aquaporin-2 (AQP2). Vasopressin regulates AQP2 in two ways to increase collecting duct water permeability (28): 1) Over a period of minutes, vasopressin stimulates trafficking of AQP2-containing vesicles to the apical region of the collecting duct cells where they fuse with the plasma membrane to increase water permeability. 2) Over a period of hours to days, vasopressin increases AQP2 protein abundance in the collecting duct cells, in part due to increased

Corresponding author: Mark A. Knepper, MD, PhD, National Institutes of Health, 10 Center Drive, Bldg 10, Room 6N260, Bethesda, MD 20892-1603. Phone: (301) 496-3187, E-mail: knep@helix.nih.gov.

transcription of the AQP2 gene. The signaling pathways involved in these responses remain incompletely understood.

In recent years, large-scale identification of proteins by mass spectrometry has become practical, and such techniques are finding increasing use in the discovery of signaling networks involved in a variety of physiological processes. An initial goal in identification of regulatory processes in a given cell type is to identify its proteome as completely as possible. To describe the proteome of the IMCD cell, we have previously carried out studies using two-dimensional (2-D) electrophoresis with protein identification by MALDI-TOF mass spectrometry (15) (34). A general drawback of 2-D electrophoresis is that certain classes of proteins are excluded from the analysis including hydrophobic proteins, proteins with very high or low molecular mass, and proteins with very high or low isoelectric points. Thus, complementary methods are needed to fully describe the set of proteins expressed in the IMCD. One viable approach combines SDS-solubilization of proteins, 1-D SDS-PAGE, in-gel trypsinization, and LC-MS/MS (1) (30), which in principle provides a way to overcome the limitations of 2-D electrophoresis. Here we use such an approach to expand the known proteome of the native rat IMCD cell. Using the new data, we present a new WWW-based "IMCD Proteome Database" that lists all proteins heretofore identified in native IMCD cells by protein mass spectrometry.

Another goal in identification of regulatory processes in a given cell type is to identify proteins whose abundances, phosphorylation states, or cellular localizations change in response to a stimulus. In a previous study using Differential In-Gel Electrophoresis (DIGE) applied in a 2-D electrophoresis format (34), we identified several proteins whose abundances in IMCD cells are altered by vasopressin. In the present study, to expand the list of IMCD proteins whose abundances are regulated by vasopressin, we use isotope-coded affinity tagging (ICAT) (11), which allows quantification in the setting of LC-MS/MS analysis. In ICAT analysis, cysteine moieties of two protein samples are derivatized via a thiol reaction using chemically identical reagents except for the substitution of some of its natural H, C, or O atoms with different stable (non-radioactive) isotopes. The resulting difference in molecular mass allows tryptic peptides from the two original samples to be distinguished and quantified by the mass spectrometer. In the current study, we use an ICAT reagent that labels cysteine side chains with a tag that contains either nine 13-C carbons or nine 12-C carbons, giving a mass difference of 9 amu for individual derivatized peptides with single cysteine. For quantification, the relative peak height for paired heavy and light peptides can be integrated over time to estimate the relative abundance of the corresponding proteins in the two original samples. Here, we employ the ICAT method for the investigation of proteins regulated in response to long-term dDAVP infusion. The animal protocol was the same as that used for our previous study, which reported DIGE-based identification of vasopressin-regulated proteins (34). Finally, we generated a protein network for vasopressin signaling in the IMCD based on previously demonstrated responses to vasopressin in native IMCD cells combined with newly hypothesized pathways based on proteomic findings of this study.

Methods

Characterization of IMCD samples versus inner medullary 'non-IMCD' samples

IMCD and non-IMCD sample preparation—Inner medullary collecting ducts were purified from rat renal inner medullas as described by Chou et al. (4). Four male Sprague Dawley rats were euthanized (NHLBI ACUC Protocol 2-KE-3). The renal inner medullas from each animal were dissected out, minced to obtain ~ 1 mm^3 pieces of tissue, and separately transferred to four glass tubes containing digestion solution (3 mg/ml collagenase B, 2000 U/ml hyaluronidase, 250 mM sucrose, 10 mM triethanolamine, pH 7.6). The suspensions were incubated at 37° C with 95% air – 5%CO_2 bubbling and continuous stirring for 60 minutes.

Low-speed centrifugation (70 xg for 10 s) was carried out to sediment the heavier IMCD cells, separating them from the lighter non-IMCD cells. The supernatants were removed and centrifuged at 1,500 xg for 10 min to pellet the non-IMCD cells. The quality of separation was examined under a dissection microscope (Wild M8, Heerbrugg, Switzerland). The IMCD and non-IMCD pellets were resuspended in 50 μl and 100 μl denaturing buffer, respectively, followed by homogenization with a sonicator probe (XL-2020 Sonicator, Misonix Inc., Farmingdale, NY). Lysates were centrifuged at 14,000 xg for 15 min to remove any insoluble material. Protein concentrations of the resulting supernatants were determined using Bradford reagent (USB Corporation, Cleveland, OH).

Quantitative LC-MS/MS analysis of IMCD vs. non-IMCD using ICAT—Samples were pooled from four rats. 250 μg each of pooled IMCD and pooled non-IMCD samples were employed for ICAT analysis as described below.

Quantitative LC-MS/MS analysis of response to long-term dDAVP administration in IMCD from Brattleboro rats

Animal procedures—Eight male Brattleboro rats (360–430 g BW; Harlan-Sprague Dawley, Indianapolis, IN) were used to investigate the response to long-term dDAVP administration in IMCD (NHLBI ACUC Protocol 2-KE-3). Four rats were infused with the V2R-selective vasopressin analog dDAVP (Rhone-Poulenc Rorer, Collegeville, PA) at 5 ng/hr for 3 days by subcutaneous osmotic minipumps (model 2001; Alzet, Palo Alto, CA). Another four rats were used as controls by receiving osmotic minipumps delivering isotonic saline solution. Rats were maintained in metabolic cages in a temperature- and humidity-controlled room with a 12:12-h light-dark cycle. They had free access to water and regular pelleted rat chow. Urine collections were made for quantitative analysis and osmolality measurement using a vapor pressure osmometer (Vapro 5520, Wescor, Logan, UT). After 3 days, the rats were killed by rapid decapitation, and inner medullas were rapidly isolated for IMCD sample preparation as described above.

Quantitative LC-MS/MS analysis of response to long-term dDAVP administration in IMCD using ICAT—400 μg of IMCD cell homogenate from pooled dDAVP samples (100 μg per rat) and pooled control samples (100 μg per rat) were employed for ICAT analysis as described below. The flow-through samples from biotin-avidin affinity purification step containing non-labeled peptides were also analyzed by nanospray LC-MS/MS to further expand the IMCD Proteome Database (See below).

Isotope-coded affinity tag (ICAT) analysis

ICAT analysis used reagents purchased from Applied Biosystems Incorporated (part number 4339035 and 4339036, Foster City, CA) and followed the manufacturer's protocol. The two samples to be compared were denatured by addition of a prescribed "denaturing buffer" (50 mM Tris, 0.1% SDS, pH 8.5) and reduced with 1.2 mM tris-(2-carboxyethyl) phosphine (TCEP) then boiled for 10 minutes. The two samples were then labeled with either ^{12}C (light) or ^{13}C (heavy) cleavable ICAT reagents (100 μg of protein per vial of ICAT reagent), respectively, for 2 hours at 37° C. Subsequently, the light and heavy ICAT reagent-labeled samples were mixed. The mixed sample was concentrated using a Speed Vac, then 5X SDS-Laemmli sample buffer was added (1:2 vol/vol Laemmli buffer:sample) prior to boiling for 10 minutes.

One-dimensional SDS-PAGE was performed using a 10% polyacrylamide Ready Gel (BioRad, Hercules, CA) to simplify the complexity of proteins in the sample. The gel was stained with colloidal coomassie blue stain (GelCode Blue Stain Reagent, G-250, Pierce Biotechnology, Rockford, IL) for 5 minutes and then destained in deionized H_2O for 1 hour. The gel was then

sliced into small blocks from the top of the stacking gel down to the dye front for a total of 16–20 blocks. Each block was minced into small pieces (1–1.5 mm^3) and placed into 1.5 ml pre-lubricated centrifuge tubes (PGC Scientifics, Frederick, MD). The gel pieces were further destained and dehydrated by incubating with 25mM NH_4HCO_3/50% acetonitrite (ACN) solution for 10 minutes three times and then the gel pieces were dried using a Speed Vac.

In-gel trypsin digestion was performed by rehydrating the gel pieces with 2.5 μg of Sequencing Grade Modified Trypsin (Promega, Madison, WI) diluted in 25mM NH_4HCO_3 solution (final concentration = 12.5 ng/μl) for 30 minutes on ice. The remaining trypsin solution was then removed and the gel pieces were briefly washed with 25 mM NH_4HCO_3 to remove excess trypsin. The gel pieces were covered with 25mM NH_4HCO_3 solution and incubated at 37° C overnight. After trypsin digestion, the peptides were extracted by incubating the gel pieces with 50% ACN/0.1% formic acid (FA) and then sonicating the gel pieces in water bath for 20 minutes. This extraction step was repeated two more times. The extracted samples were dried by a Speed Vac and then reconstituted with 500 μl 2X PBS (20 mM NaH_2PO_4, 300 mM NaCl, pH 7.2) before proceeded to purify the ICAT reagent-labeled peptides using biotin-avidin affinity purification step as recommended by the manufacturer (ICAT Cartridge – Avidin, Applied Biosystems, Foster City, CA). The affinity tag portion of ICAT reagent was then cleaved off using cleaving reagent containing concentrated trifluoroacetic acid (TFA) for 2 hours at 37° C. The ICAT reagent-labeled peptides were concentrated and cleaned up using ZipTip C18 pipette tip and then dried and reconstituted with 0.1% FA before analysis by nanospray LC-MS/MS.

Validation of ICAT Method—Two 25 μg BSA samples labeled with heavy or light ICAT reagents were prepared as described above. The two samples were denatured, reduced, derivatized with heavy or light reagents, and mixed in specified ratios (either 1:1 or 1:2). The mixed samples were digested with trypsin (62.5 ng/μl) in solution at 37° C overnight (SDS gel separation was not performed on BSA samples in contrast to other studies in this paper). The tryptic peptides were separated from the TCEP, SDS, and excess ICAT reagents by cation exchange chromatography (ICAT Cartridge – Cation Exchange, Applied Biosystems, Foster City, CA). The biotin-containing derivatized peptides were affinity purified and cleaved as described under ***"ICAT"*** above. MALDI-TOF/TOF analysis (4700 Proteomics Analyzer, Applied Biosystems, Foster City, CA) was performed on the 1:1 and 1:2 mixed samples. Mascot (Matrix Science Inc., Boston, MA) software was used to search raw data files. GPS Explorer (Applied Biosystems, Foster City, CA) software was used to quantify the ICAT results. Results were confirmed with nanospray LC-MS/MS analysis (LCQ Deca XP Plus, Thermo Finnigan, San Jose, CA) performed on the 1:1 mixed sample.

Nanospray LC-MS/MS—One-dimensional LC-MS/MS using a modified configuration of the ProteomeX 2D LC/MS workstation was employed for ICAT analysis (LCQ Deca XP Plus, Thermo Finnigan, San Jose, CA). Chromatographic separation of peptides was accomplished using two Zorbax 300SB-C18 peptide traps (Agilent Technologies, Wilminton, DE), working in alternating fashion (replacing the standard strong cation exchange and reverse phase columns), while the standard ESI source was replaced by a nanospray ionization source and a reversed-phase PicoFrit^{TM} column (BioBasic C18, 75 mm x 10cm, tip = 15 μm, New Objective, Woburn, MA). The peptides were loaded onto the traps in alternating fashion using an autosampler. After washing with 0.1% formic acid, the peptides were eluted by 0–60% solvent B in solvent A (A = 0.1% formic acid; B = acetonitrile) in 30 min at a flow rate of about 200 nl/min. The flow-through samples from the avidin affinity column were analyzed using a LTQ linear trap tandem mass spectrometer (Thermo Finnigan, San Jose, CA).

Inclusion criteria for identified peptides—The mass/charge (m/z) ratios of peptides and their fragmented ions were recorded by a method that allows the acquisition of three (LCQ

mass spectrometer) or five (LTQ mass spectrometer) MS2 scans following each full MS scan. The raw datafiles were searched against the rat protein database from NCBI using the BioWorks 3.1 software (Thermo Finnigan, San Jose, CA) based on the Sequest algorithm. The search parameters included the following: precursor-ion mass accuracy = 3.0 amu (LCQ) or 1.5 amu (LTQ); fragment-ion mass accuracy = 1.0 amu (LCQ) or 0.0 amu (LTQ); modification allowed for addition of light or heavy ICAT reagents on cysteine; and 2 missed cleavages allowed. After the peptide sequence and protein identification from BioWorks software was carried out, the identified peptide sequences were initially filtered using the cross correlation score (Xcorr) at the following threshold: Xcorr > 1.5 for 1+ ion, 2.0 for 2+ ion, and 2.5 for 3+ ion.

For each identified ICAT reagent-labeled peptide that passed the filter threshold, proteins identified were selected if they achieved the following criteria: 1) peptide sequence had the highest Xcorr score for a particular collision-induced dissociation (CID) spectrum; 2) peptide sequence had a delta normalized correlation score ≥ 0.08; and 3) peptide sequence had good quality CID spectra by visual inspection. All identified peptide sequences were searched using BLAST to obtain the best possible unique protein ID, thus eliminating redundant annotations.

For each identified peptide from the flow-through samples that passed the initial filter threshold, proteins identified from two or more different peptides were selected if they achieved the following criteria: 1) peptide sequence had the highest Xcorr score for a particular CID spectrum; 2) peptide sequence had a delta normalized correlation score ≥ 0.08; and 3) peptide sequence had the ranking of the preliminary raw score ≤ 10.

Quantification of ICAT results—The XPRESS algorithm implemented in BioWorks 3.1 software was used to calculate the ICAT ratio of each identified ICAT reagent-labeled peptide. The parameters using for this calculation were 1) light/heavy ICAT reagent-labeled cysteine mass difference = 9 amu; 2) mass tolerance = 1.0–1.5 amu; and 3) scan window = 60 full MS scans. Manually inspection of reconstructed ion chromatogram was performed to validate the quantification results.

Immunoblotting

Immunoblotting was performed as described (7). Briefly, proteins were resolved by SDS-PAGE gel electrophoresis on 7.5%, 10%, or 12% polyacrylamide gels and transferred electrophoretically onto nitrocellulose membranes. The membranes were then blocked with 5% nonfat dry milk in immunoblot wash buffer (42 mM Na_2HPO_4, 8 mM NaH_2PO_4, 150 mM NaCl, and 0.05% Tween 20, pH 7.5), rinsed and probed with primary antibody overnight at room temperature. After washing, blots were incubated with species-specific secondary antibodies conjugated to horseradish peroxidase. After the final wash, antibody binding was visualized by chemiluminescence (LumiGLO; KPL, Gaithersburg, MD) using light sensitive film developed on the Kodak M35A X-OMAT Processor.

Antibodies—The rabbit polyclonal antibodies to AQP1, AQP2, β-ENaC, and γ -ENaC were previously generated in our laboratory (21) and a rabbit polyclonal antibody to the α-1 subunit of Na/K-ATPase was newly prepared using a synthetic peptide (sequence: CDEVRKLIIRRRPGGWVEKETYY) conjugated to keyhole limpit hemocyanin. The anti-Myosin IIA rabbit polyclonal was a gift of Dr. Robert Adelstein (NHLBI, Bethesda, MD). The commercial antibodies used are listed as follows: β-Actin (rabbit polyclonal, 4967, Cell Signaling Technology, Beverly, MA); Aldose reductase (goat polyclonal, sc-17735), Annexin II (goat polyclonal, sc-1924), Annexin IV (goat polyclonal, sc-1930), Cathepsin D (goat polyclonal, sc-6486), HSP70 (goat polyclonal, sc-1060), RhoA (mouse monoclonal, sc-418), RhoGDI (rabbit polyclonal, sc-360), RACK1 (mouse monoclonal, sc-17754), Rap1 (rabbit polyclonal, sc-65), and Cdc42 (rabbit polyclonal, sc-87) from Santa Cruz Biotechnology (Santa

Cruz, CA); Transglutaminase 2 (goat polyclonal, 06-471, Upstate, Waltham, MA); GAPDH (mouse monoclonal, NB 300–221, Novus Biologicals, Littleton, CO); β-Spectrin II (mouse monoclonal, 612562, BD Biosciences Pharmingen, San Jose, CA); GRP58 (rabbit polyclonal, P7496, Sigma-Aldrich, St. Louis, MO); and Syntaxin-7 (rabbit polyclonal, 110 072, Synaptic Systems GmbH, Goettingen, Germany).

Bioinformatic network analysis

Proteins regulated in response to long-term dDAVP administration that were validated by immunoblotting were analyzed further by bioinformatic network analysis. This analysis used the core signaling pathway downstream from V2R occupation in IMCD demonstrated by previous studies (8) (29) (14) (3) (5) (23) (18) (13) (36) (2) as the core network. The connections between the newly identified proteins and the core network were created through manual and computer-aided literature searching (Ingenuity Pathway Analysis [IPA], Ingenuity Systems, Mountain View, CA, www.ingenuity.com; and MetaCore, GeneGo, St. Joseph, MI, www.genego.com). The networks are displayed graphically as nodes (individual proteins or molecules) and edges (the biological interactions between the nodes).

IMCD Proteome Database

A database of all proteins identified by protein mass spectrometry in inner medullary collecting duct in this study and prior studies (15) (34) (1) (16) was constructed as an Excel spreadsheet. The spreadsheet was used to generate HTML files which are posted on a central server at URL: http://dir.nhlbi.nih.gov/papers/lkem/imcd/index.htm. The database is limited to protein mass spectrometry data from freshly isolated inner medullary collecting ducts of rats prepared as above.

Results

Validation of ICAT Method

As a preliminary test of the validity of the ICAT method in our setting, we have carried out labeling of samples containing differing amounts of bovine serum albumin (BSA). Figure 1A shows examples of MALDI-TOF spectra with 1:1 and 1:2 ratios of BSA labeled with the light ICAT reagent (^{12}C) and the heavy ICAT reagent (^{13}C), respectively. As can be seen, the peak heights for various BSA peptides were approximately in proportion the relative amounts of BSA in the two samples. Figure 1B demonstrates the reconstructed ion chromatograms from LC-MS/MS analysis of a BSA tryptic peptide (sequence: LKPDPNTLCDEFK) labeled with light:heavy ICAT reagent in 1:1 ratio. The area under the entire envelope was used for measuring the ICAT ratio. Figure 1C shows data from LC-MS/MS showing a histogram of the ^{12}C /^{13}C ratios for all BSA peptides when a 1:1 ratio was utilized. For 53 peptides, the mean ratio was 1.04 and the standard deviation was 0.19.

Comparison of IMCD samples with inner medullary ‘non-IMCD’ samples

To analyze the IMCD proteome and its response to vasopressin, it is necessary to isolate IMCD cells from the renal inner medulla of rat. This is done by a low-speed centrifugation technique utilized previously in proteomic analyses of the inner medulla (15) (34) (described in Methods). This technique yields purified IMCD cells in one sample and the residual cell types from the inner medulla in the other sample (termed ‘non-IMCD’ cells). Figure 2 shows an immunoblot characterization of these cell fractions. As can be seen, for four different preparations labeled A-D, the collecting duct marker aquaporin-2 (AQP2) was strongly enriched in the IMCD fraction. The AQP2 band density ratio for the IMCD fraction: non-IMCD fraction was 259 ± 131 (mean ± SD [n = 4]). The descending limb of Henle/vasa recta marker aquaporin-1 (AQP1) was strongly de-enriched in the IMCD fraction. The band density ratio for the IMCD fraction:

non-IMCD fraction was 0.09 ± 0.10 (mean ± SD [n = 4]). Thus, the IMCD purification was successful.

Quantitative LC-MS/MS analysis of IMCD vs. non-IMCD proteome using ICAT

Initial experiments (Figure 3) were carried out to test the ability of ICAT to quantify protein abundance differences in biological tissues. This experiment compared IMCD samples (250 μg protein pooled from 4 animals; labeled with ^{12}C reagent) vs. non-IMCD inner medullary cell samples (250 μg protein pooled from 4 animals; labeled with ^{13}C reagent). Table 1 gives the ^{12}C:^{13}C ratios for proteins (n = 44) for which two or more unique peptides were identified. Figure 4 shows a plot of the correlation of ratios obtained with ICAT in this study vs. those obtained by DIGE in our previous study using the same technique for separating IMCD tubules from non-IMCD tubules. The specific proteins plotted in Figure 4 are indicated in Table 1. In general, most of the 17 proteins identified both in the ICAT and DIGE studies changed in the same direction in both studies. Lack of correlation for the four proteins that changed in opposite directions can potentially be attributed to post-translational modifications, which can produce changes in DIGE due to shifts in the position of the spots in the 2-D gels while not affecting the ratio obtained by ICAT. Full results for all proteins identified regardless of the number of peptide sequences found (n = 89) are presented in Supplementary Table 1. All single-peptide identifications were checked by manually observing the associated spectra. A summary of the types of proteins identified are presented in Figure 5. IMCD:non-IMCD abundance ratios using ICAT were in the range 0.03 to 7.69 (Supplementary Table 1), similar to the range seen in previous studies using DIGE (15).

To test further the fidelity of the ICAT quantification in this experiment, we carried out semiquantitative immunoblotting for 10 of the proteins for which we could obtain suitable antibodies (Figure 6). The immunoblots shown were carried out using aliquots of the same samples used in the ICAT experiment except that the immunoblotting samples were not pooled. Thus, each lane corresponds to an IMCD sample from a different animal. In general, the immunoblotting results paralleled the ICAT results, although the specific IMCD:non-IMCD ratios differed in several cases. In general, we conclude from comparison with DIGE data and immunoblotting data that ICAT can successful identify and quantify differences in protein abundance in tissue samples.

Quantitative LC-MS/MS analysis of response to long-term dDAVP administration in IMCD from Brattleboro rats

To identify IMCD proteins whose abundances are altered in response to long-term elevations of circulating vasopressin levels, we carried out experiments using Brattleboro rats, which have no endogenous vasopressin. Brattleboro rats were infused with either the V2R-selective vasopressin analog dDAVP (5 ng/hr for 3 days in osmotic minipumps) or vehicle (for 3 days). Urine output and urine osmolality as a function of infusion period are shown in Figure 7. As typically seen, the urinary output fell and the urinary osmolality rose substantially in response to dDAVP infusion. The animals were euthanized after 3 days, IMCD suspensions were prepared and a portion of these samples were used for semi-quantitative immunoblotting to confirm the action of the infused dDAVP (Figure 8). There was a marked increase in the abundance of AQP2 in accord with previous observations (7). In addition, there was a marked increase in the abundance of the γ-subunit of the epithelial sodium channel (ENaC) and a trend toward an increase in β-ENaC, similar to the changes previously recorded in the cortical and outer medullary collecting ducts (9). Thus, we conclude that the infused dDAVP was effective in stimulating the expected long-term responses in the IMCD.

We used the same samples to carry out ICAT analysis of the dDAVP response using a Thermo Finnigan LCQ LC-MS/MS system. This experiment compared IMCD proteins from dDAVP-

treated animals (400 μg protein pooled from 4 animals) vs. IMCD proteins from vehicle-infused animals (400 μg protein pooled from 4 animals) as summarized in Figure 9. A total of 165 proteins were identified which had high quality spectra for which ^{13}C:^{12}C ratios could be determined (full results for all proteins identified are presented in Supplementary Table 2). Table 2 summarizes the proteins with dDAVP:control (^{13}C:^{12}C) ratios that were significantly different from unity based on observations in 3 or more quantifiable spectra corresponding to the same protein. Figure 10 shows a classification of these proteins based on the Collecting Duct Database (CDDB) identifiers (24) (http://cddb.nhlbi.nih.gov/cddb/). Cytoskeletal proteins and linkers/molecular motors (n = 7), biosynthetic proteins (n = 5), and proteins involved in energy metabolism (n = 4) are the major types of proteins that appeared to respond to the long-term vasopressin action.

In order to confirm the ICAT ratios, immunoblots were performed on as many proteins as possible for which validated antibodies are available. Figure 11A shows immunoblotting results for 16 selected proteins quantified by ICAT. As can be seen, the immunoblots confirmed the direction of change determined by ICAT in 14 of 16 cases. The two proteins for which the direction of change was not verified (RACK1 and Rap1) were proteins that have only one ICAT ratio value. The proteins that significantly changed in abundance based on immunoblotting were cathepsin D (increased), glyceraldehyde-3-phosphate dehydrogenase (increased), heat shock 70kDa protein (increased), Rap1 (decreased), and syntaxin-7 (increased). As can be seen in Figure 11B, there was a general correlation between the magnitudes of abundance change as determined by immunoblotting and ICAT, which improved when proteins identified on the basis of only one peptide were excluded.

Figure 12 shows a bioinformatic network representing the relationships between the core signaling pathway downstream from V2R occupation in IMCD demonstrated by previous studies (8) (29) (14) (3) (5) (23) (18) (13) (36) (2) and the five proteins regulated in response to long-term dDAVP administration that were validated by immunoblotting in this study (see above). The connections between the newly identified proteins and the core network were generated through manual and computer-aided literature searching (IPA and MetaCore, see Methods). Supplementary Table 3 describes the interactions between parent nodes and child nodes in the bioinformatic network. Supplementary Table 4 demonstrates protein names and references documenting the presence of the individual proteins in IMCD.

Protein identifications in flow-through fractions of biotin-avidin affinity purification in dDAVP-infusion experiment

The flow-through samples from the biotin-avidin affinity purification step containing non-labeled IMCD peptides were analyzed by a LTQ linear trap tandem mass spectrometer to expand the number of the IMCD proteins identified. Supplementary Table 5 shows IMCD proteins identified with 2 or more unique peptides (n = 630).

IMCD Proteome Database

With this study, we have now completed 5 distinct studies revealing elements of the IMCD proteome (15) (34) (1) (16). To provide a resource making these data generally available, we have created an “IMCD Proteome Database” that includes all proteins (presently n = 848) identified in IMCD cells in these studies. This database is accessible at http://dir.nhlbi.nih.gov/papers/lkem/imcd/index.htm. The database will be updated further as new proteins are identified, and is limited to proteins identified by mass spectrometry in freshly isolated IMCD cells using high stringency filters to avoid false-positive identifications. Figure 13 represents the distribution of proteins currently available in the IMCD Proteome Database categorized by the Collecting Duct Database (CDDB) identifiers (24).

Discussion

In this study we have used LC-MS/MS-based mass spectrometry to investigate the proteome of the IMCD cell, and how it is altered in response to long-term vasopressin administration in rats. We present a WWW-based "IMCD Proteome Database", containing all IMCD proteins identified in this study (n = 704) and prior MS-based identification studies (n = 301). Because 157 proteins are present in both lists, the current total count of proteins in the IMCD Proteome Database is 848. An important initial goal in this study was to validate the use of ICAT for large-scale quantification of proteins in isolated IMCD cells from kidney. We ultimately used ICAT to identify proteins that are increased or decreased in abundance in response to the long-term infusion of the V2 vasopressin receptor-selective agonist dDAVP. ICAT has been most successful in the quantitative proteomic study of regulatory processes in yeast (11), in which very large numbers of cells can be harvested. For example, a study of the response of the yeast proteome to salt stress, a total of 800 μg was used for the starting material (25). In our initial studies, we found that similar amounts of kidney protein must be analyzed in order to identify all but the most abundant proteins. Thus, ICAT (as applied in the present study) is relatively lacking in sensitivity, a factor that limits its practicality in some types of experiments, e.g. those involving prefractionation which may yield relatively small amounts of protein for analysis, or analysis of very small tissue elements such as those that may be harvested from developing embryos. In addition, the method is limited by the fact that it depends on labeling of cysteines. Consequently the method will be blind to many proteins that do not have cysteine moieties in tryptic peptides in a size range that is visible to the mass spectrometer. This includes aquaporin-1 and aquaporin-2, for example, proteins that are of considerable physiological importance in the renal inner medulla. Furthermore, as illustrated in Figure 1C, the method is subject to considerable error even for relatively abundant proteins. Nevertheless, ICAT performed successfully in quantification of many relatively abundant proteins in the whole cell analyses presented in this paper, matching well with results from either immunoblotting or DIGE analysis.

One potential advantage of ICAT and LC-MS/MS in general over DIGE and other 2-D gel based methods is the ability to quantify integral membrane proteins. In the present study, 9 out of the total of 165 proteins (5.5%) were integral membrane proteins in the dDAVP infusion study, while 7 out of 89 proteins (7.9%) were integral membrane proteins in the experiment in which we compared IMCD vs. non-IMCD cell fractions. In contrast, our previous studies (15) using DIGE for quantification identified 2 integral membrane proteins out of a total of 125 proteins (1.6%). Thus, our results indicate that the combination of ICAT and LC-MS/MS indeed gives a greater yield of integral membrane proteins than does DIGE. Overall, we believe that 2-D DIGE and ICAT with LC-MS/MS are complementary methods that, when used in combination, will give a much higher yield of successfully identified and quantified proteins than either technique alone.

Another important issue addressed by our study is the need to isolate a tissue fraction that is as homogeneous as possible from the perspective of cell type. As illustrated in Table 1, many proteins are differentially expressed in IMCD and non-IMCD elements of the renal medulla. Attempts to quantify protein changes in response to a physiological perturbation based on analysis of whole inner medulla may therefore be reflective of IMCD cells or of non-IMCD cells. Furthermore, responses in IMCD cells may be masked by opposite changes in other cell types.

An important objective of the current study was to identify proteins in IMCD cells of rat whose abundances change in response to a long-term (3 day) infusion of the vasopressin analog dDAVP. As illustrated in Table 2, some proteins increased and some proteins decreased in abundance in response to dDAVP. The protein list in Table 2 can be considered a presumptive

list of proteins regulated in response to long-term dDAVP administration. Members of this list can be considered targets for further hypothesis-driven investigation. The functional classification of these proteins was annotated using a terminology based on that of the Collecting Duct Database (CDDB) (24) (http://cddb.nhlbi.nih.gov/cddb/). As shown in Figure 10, cytoskeletal proteins and linkers/molecular motors, biosynthetic proteins, and proteins involved in energy metabolism appear to be the major types of proteins that responded to the long-term vasopressin action. Sixteen of the proteins that were quantified by ICAT analysis were investigated further by semiquantitative immunoblotting, which confirmed the direction of change demonstrated by ICAT in 14 of 16 proteins. The proteins that significantly changed in abundance based on immunoblotting were cathepsin D, glyceraldehyde-3-phosphate dehydrogenase (GAPDH), heat shock 70kDa protein (HSP70), Rap1, and syntaxin-7. The responses were analyzed further by carrying out network analysis incorporating the core signaling pathway downstream from V2R occupation in IMCD demonstrated by previous studies (8) (29) (14) (3) (5) (23) (18) (13) (36) (2) and the five proteins validated by immunoblotting as described above. The functional interactions between proteins were culled from the literature through manual and computer-aided searching (IPA and MetaCore).

Overall, this study adds to the number of proteins known to populate the “IMCD Proteome”. A long-term goal of our studies is to identify as many members of the IMCD proteome as possible to provide a database of information that will facilitate systems biological analysis (mathematical modeling) of cellular processes in IMCD cells. The database as it exists currently is available at http://dir.nhlbi.nih.gov/papers/lkem/imcd/index.htm and reflects IMCD proteins identified from 5 distinct studies (15) (34) (1) (16) and this study.

The remainder of the discussion will focus on the component of the network described in Figure 12. The existing portion of the the network (nodes indicated in gray) describe well documented elements of vasopressin signaling demonstrated in prior papers. One objective of proteomics studies such as this one is to generate new hypotheses that can lead to critical experiments regarding signaling pathways. The new proteins, indicated in red, constitute hypothetical extensions of the existing network, linked to the existing network directly or via additional IMCD proteins indicated by uncolored nodes. All proteins in Figure 12 have been specifically and unequivocally demonstrated to be expressed in the IMCD (see IMCD Proteome Database discussed in previous paragraph).

Syntaxin-7

Syntaxins are so-called t-SNARE proteins that together with SNAP23 or SNAP25 and a synaptobrevin isoform, forms a heterotrimeric coiled-coil SNARE complex that plays a critical role in vesicle fusion (20). Previous studies (27) (26) have demonstrated two syntaxins expressed in the IMCD, viz. syntaxin-3 and syntaxin-4, both of which are plasma membrane syntaxins. Subsequently, several endosomal syntaxins including syntaxin-7, syntaxin-12 and syntaxin-13 were demonstrated in AQP2-containing vesicles in IMCD cells (1). In the present study, the presence of syntaxin-7 in IMCD was confirmed and its abundance was found to be upregulated in response to dDAVP infusion in Brattleboro rats. Syntaxin-7 is thought to be localized to either the early (31) or late (35) endosomal compartment. As previously described, AQP2 is regulated by vasopressin through separate processes which separately regulate exocytosis and endocytosis of the water channel (22). Conceivably, upregulation of syntaxin-7 abundance could be a component of the process regulating endocytosis.

Rap1

Rap1 is a small Ras-like GTP-binding protein that has been implicated in several regulatory processes in cells including activation of the MAP kinase pathway and mobilization of intracellular calcium through activation of calcium-induced calcium release channels in the

endoplasmic reticulum (12). Rap1 is the downstream target of Epac, a guanine nucleotide exchange factor (GEF) that binds to and activates Rap1. Epac is a direct target for cAMP, which activates it. Hence, we can hypothesize that cAMP-induced calcium mobilization may be mediated by Epac and Rap1 as previously demonstrated in pancreatic β-cells (19). This hypothesis is directly testable since Epac-selective cAMP analogues are now commercially available. In the present studies, immunoblotting demonstrated an apparent decrease in Rap1 protein abundance in response to dDAVP, an effect which could attenuate the proposed role of Epac and Rap1. Rap1 has been previously demonstrated to be present in AQP2-containing vesicles in IMCD cells (1).

GAPDH

An increase in the IMCD abundance of GAPDH was demonstrated in the present study in response to dDAVP infusion, consistent with the prior studies showing an increase in GAPDH mRNA in response to dDAVP in the inner medulla (2). GAPDH is often considered a housekeeping protein and it is often used to normalize results from mRNA or protein measurements. However, our results indicating that GAPDH abundance can be regulated suggests that other normalizing measures should be sought. GAPDH is known as a glycolytic enzyme, but a variety of other functions have been demonstrated including a catalytic role in membrane fusion (33) (10). Thus, increases in GAPDH abundance could be highly relevant to the regulation of aquaporin-2 trafficking. GAPDH has been demonstrated to be a binding partner for tubulin, which inhibits GAPDH-catalyzed membrane fusion activity (10).

HSP70

This study also demonstrated a dDAVP-induced increase in HSP70 expression in the IMCD, confirming previous results from DIGE-based studies (34). HSP70 is an adundant molecular chaperone. It has been demonstrated to be increased in abundance in cultured MDCK cells (6) in response to increased tonicity, leading us to speculate that the increase in HSP70 expression in the present study is a response to altered inner medullary tonicity rather than to dDAVP itself.

Cathepsin D

This is a renin-like proteolytic enzyme that was also demonstrated to be upregulated in response to dDAVP in the IMCD, confirming the findings of DIGE-based studies (34). This protein has also been demonstrated to be transcriptionally regulated by p53 (32), a protein that has been recently implicated in IMCD signaling in association with vasopressin escape (17).

References

1. Barile M, Pisitkun T, Yu MJ, Chou CL, Verbalis MJ, Shen RF, Knepper MA. Large Scale Protein Identification in Intracellular Aquaporin-2 Vesicles from Renal Inner Medullary Collecting Duct. Mol Cell Proteomics 2005;4:1095–1106. [PubMed: 15905145]
2. Brooks HL, Ageloff S, Kwon TH, Brandt W, Terris JM, Seth A, Michea L, Nielsen S, Fenton R, Knepper MA. cDNA array identification of genes regulated in rat renal medulla in response to vasopressin infusion. Am J Physiol Renal Physiol 2003;284:F218–F228. [PubMed: 12388413]
3. Chou CL, Christensen BM, Frische S, Vorum H, Desai RA, Hoffert JD, de Lanerolle P, Nielsen S, Knepper MA. Non-muscle myosin II and myosin light chain kinase are downstream targets for vasopressin signaling in the renal collecting duct. J Biol Chem 2004;279:49026–49035. [PubMed: 15347643]
4. Chou CL, DiGiovanni SR, Luther A, Lolait SJ, Knepper MA. Oxytocin as an antidiuretic hormone. II. Role of V2 vasopressin receptor. Am J Physiol 1995;269:F78–F85. [PubMed: 7631834]

5. Chou CL, Yip KP, Michea L, Kador K, Ferraris J, Wade JB, Knepper MA. Regulation of aquaporin-2 trafficking by vasopressin in renal collecting duct: Roles of ryanodine-sensitive Ca^{2+} stores and calmodulin. J Biol Chem 2000;275:36839–36846. [PubMed: 10973964]
6. Cohen DM, Wasserman JC, Gullans SR. Immediate early gene and HSP70 expression in hyperosmotic stress in MDCK cells. Am J Physiol 1991;261:C594–C601. [PubMed: 1718164]
7. DiGiovanni SR, Nielsen S, Christensen EI, Knepper MA. Regulation of collecting duct water channel expression by vasopressin in Brattleboro rat. Proc Natl Acad Sci U S A 1994;91:8984–8988. [PubMed: 7522327]
8. Ecelbarger CA, Chou CL, Lolait SJ, Knepper MA, DiGiovanni SR. Evidence for dual signaling pathways for V2 vasopressin receptor in rat inner medullary collecting duct. Am J Physiol 1996;270:F623–F633. [PubMed: 8967340]
9. Ecelbarger CA, Kim GH, Terris J, Masilamani S, Mitchell C, Reyes I, Verbalis JG, Knepper MA. Vasopressin-mediated regulation of ENaC abundance in rat kidney. Am J Physiol Renal Physiol 2000;279:F46–F53. [PubMed: 10894786]
10. Glaser PE, Han X, Gross RW. Tubulin is the endogenous inhibitor of the glyceraldehyde 3-phosphate dehydrogenase isoform that catalyzes membrane fusion: Implications for the coordinated regulation of glycolysis and membrane fusion. Proc Natl Acad Sci U S A 2002;99:14104–14109. [PubMed: 12381782]
11. Gygi SP, Rist B, Gerber SA, Turecek F, Gelb MH, Aebersold R. Quantitative analysis of complex protein mixtures using isotope-coded affinity tags. Nat Biotechnol 1999;17:994–999. [PubMed: 10504701]
12. Hattori M, Minato N. Rap1 GTPase: functions, regulation, and malignancy. J Biochem (Tokyo) 2003;134:479–484. [PubMed: 14607972]
13. Henn V, Edemir B, Stefan E, Wiesner B, Lorenz D, Theilig F, Schmitt R, Vossebein L, Tamma G, Beyermann M, Krause E, Herberg FW, Valenti G, Bachmann S, Rosenthal W, Klussmann E. Identification of a novel A-kinase anchoring protein 18 isoform and evidence for its role in the vasopressin-induced aquaporin-2 shuttle in renal principal cells. J Biol Chem 2004;279:26654–26665. [PubMed: 15037626]
14. Hoffert JD, Chou CL, Fenton RA, Knepper MA. Calmodulin is required for vasopressin-stimulated increase in cyclic AMP production in inner medullary collecting duct. J Biol Chem 2005;280:13624–13630. [PubMed: 15710610]
15. Hoffert JD, van Balkom BW, Chou CL, Knepper MA. Application of difference gel electrophoresis to the identification of inner medullary collecting duct proteins. Am J Physiol Renal Physiol 2004;286:F170–F179. [PubMed: 12965894]
16. **Hoorn EJ, Hoffert JD and Knepper MA** Combined Proteomics and Pathways Analysis of Collecting Duct Reveals a Protein Regulatory Network Activated in Vasopressin Escape. *J Am Soc Nephrol* 2005.
17. Hoorn EJ, Hoffert JD, Knepper MA. Combined proteomics and pathways analysis of collecting duct reveals a protein regulatory network activated in vasopressin escape. J Am Soc Nephrol 2005;16:2852–2863. [PubMed: 16079266]
18. Jo I, Ward DT, Baum MA, Scott JD, Coghlan VM, Hammond TG, Harris HW. AQP2 is a substrate for endogenous PP2B activity within an inner medullary AKAP-signaling complex. Am J Physiol Renal Physiol 2001;281:F958–F965. [PubMed: 11592953]
19. Kang G, Chepurny OG, Rindler MJ, Collis L, Chepurny Z, Li WH, Harbeck M, Roe MW, Holz GG. A cAMP and Ca2+ coincidence detector in support of Ca2+-induced Ca2+ release in mouse pancreatic beta cells. J Physiol 2005;566:173–188. [PubMed: 15860526]
20. Knepper MA, Inoue T. Regulation of aquaporin-2 water channel trafficking by vasopressin. Curr Opin Cell Biol 1997;9:560–564. [PubMed: 9261056]
21. Knepper MA, Masilamani S. Targeted proteomics in the kidney using ensembles of antibodies. Acta Physiol Scand 2001;173:11–21. [PubMed: 11678722]
22. Knepper MA, Nielsen S. Kinetic model of water and urea permeability regulation by vasopressin in collecting duct. Am J Physiol 1993;265:F214–F224. [PubMed: 8396343]

23. Kuwahara M, Fushimi K, Terada Y, Bai L, Marumo F, Sasaki S. cAMP-dependent phosphorylation stimulates water permeability of aquaporin-collecting duct water channel protein expressed in Xenopus oocytes. J Biol Chem 1995;270:10384–10387. [PubMed: 7537730]
24. Legato J, Knepper MA, Star RA, Mejia R. Database for renal collecting duct regulatory and transporter proteins. Physiol Genomics 2003;13:179–181. [PubMed: 12646711]
25. Li J, Steen H, Gygi SP. Protein Profiling with Cleavable Isotope-coded Affinity Tag (cICAT) Reagents: The Yeast Salinity Stress Response. Mol Cell Proteomics 2003;2:1198–1204. [PubMed: 14506205]
26. Mandon B, Chou CL, Nielsen S, Knepper MA. Syntaxin-4 is localized to the apical plasma membrane of rat renal collecting duct cells: Possible role in aquaporin-2 trafficking. J Clin Invest 1996;98:906–913. [PubMed: 8770861]
27. Mandon B, Nielsen S, Kishore BK, Knepper MA. Expression of syntaxins in rat kidney. Am J Physiol 1997;273:F718–F730. [PubMed: 9374835]
28. Nielsen S, Frokiaer J, Marples D, Kwon TH, Agre P, Knepper MA. Aquaporins in the kidney: from molecules to medicine. Physiol Rev 2002;82:205–244. [PubMed: 11773613]
29. Noda Y, Sasaki S. Trafficking mechanism of water channel aquaporin-2. Biol Cell 2005;97:885–892. [PubMed: 16293109]
30. Pisitkun T, Shen RF, Knepper MA. Identification and proteomic profiling of exosomes in human urine. Proc Natl Acad Sci U S A 2004;101:13368–13373. [PubMed: 15326289]
31. Prekeris R, Yang B, Oorschot V, Klumperman J, Scheller RH. Differential roles of syntaxin 7 and syntaxin 8 in endosomal trafficking. Mol Biol Cell 1999;10:3891–3908. [PubMed: 10564279]
32. Sun Y, Wicha M, Leopold WR. Regulation of metastasis-related gene expression by p53: a potential clinical implication. Mol Carcinog 1999;24:25–28. [PubMed: 10029407]
33. Tisdale EJ, Kelly C, Artalejo CR. Glyceraldehyde-3-phosphate dehydrogenase interacts with Rab2 and plays an essential role in endoplasmic reticulum to Golgi transport exclusive of its glycolytic activity. J Biol Chem 2004;279:54046–54052. [PubMed: 15485821]
34. van Balkom BW, Hoffert JD, Chou CL, Knepper MA. Proteomic analysis of long-term vasopressin action in the inner medullary collecting duct of the Brattleboro rat. Am J Physiol Renal Physiol 2004;286:F216–F224. [PubMed: 14532164]
35. Ward DM, Pevsner J, Scullion MA, Vaughn M, Kaplan J. Syntaxin 7 and VAMP-7 are soluble N-ethylmaleimide-sensitive factor attachment protein receptors required for late endosome-lysosome and homotypic lysosome fusion in alveolar macrophages. Mol Biol Cell 2000;11:2327–2333. [PubMed: 10888671]
36. Yamaki M, McIntyre S, Rassier ME, Schwartz JH, Dousa TP. Cyclic 3',5'-nucleotide diesterases in dynamics of cAMP and cGMP in rat collecting duct cells. Am J Physiol 1992;262:F957–F964. [PubMed: 1320333]

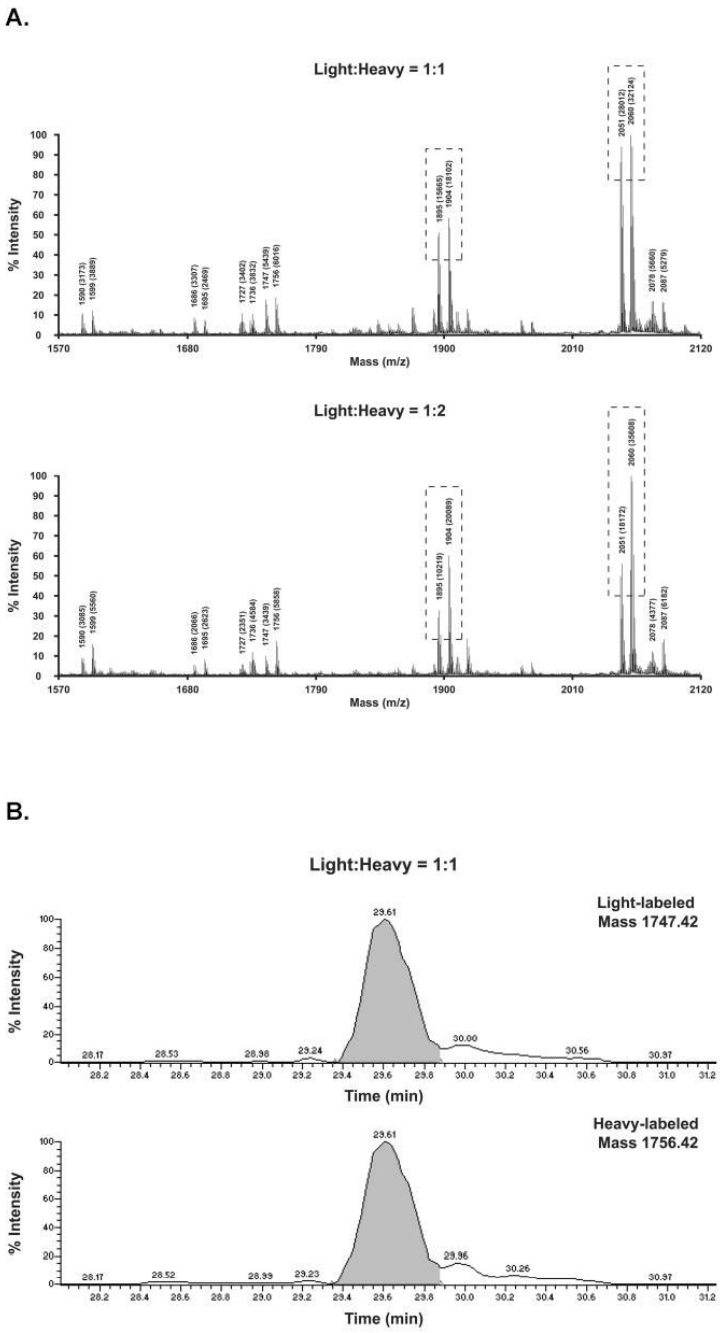

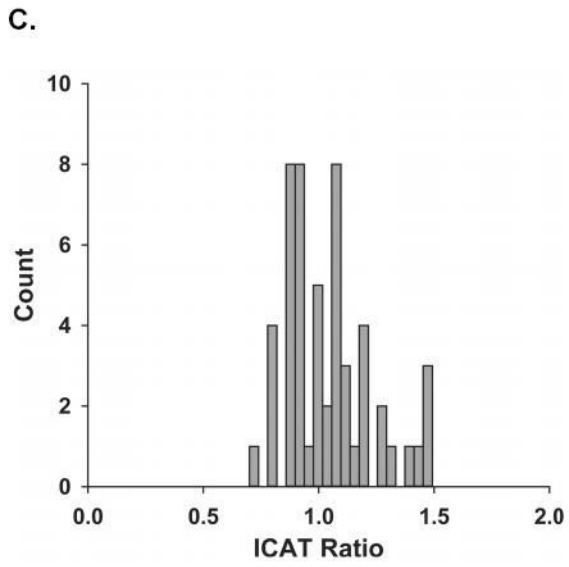

Figure 1.

A) MALDI-TOF spectra of bovine serum albumin (BSA) tryptic peptides from 1:1 mixing (upper panel) and 1:2 mixing (lower panel) of light:heavy ICAT reagent-labeled BSA. Dashed boxes highlight some pairs of typical ICAT spectra containing 2 identical peptide peaks, one labeled with light reagent (left side) and one labeled with heavy reagent (right side), both of which have mass difference of 9 amu. The relative intensities of these pairs correlate well with the mixing ratio (quantitative errors of 15.5% and 7.5% for 1:1 mixing and 1:2 mixing, respectively). Numbers above each peak indicate m/z and area under the peak (in parenthesis). **B**) Reconstructed ion chromatograms from LC-MS/MS analysis of a BSA tryptic peptide (sequence: LKPDPNTLCDEFK) labeled with light ICAT reagent (upper panel) and heavy ICAT reagent (lower panel) in 1:1 ratio. A “reconstructed ion chromatogram” shows the peak height for an individual peptide collected from multiple spectra over time during elution from the HPLC column. The area under the entire envelope (grey area) was used for the quantification of ICAT ratio. **C**) Histogram demonstrating LC-MS/MS ICAT ratios of 1:1 mixing of light:heavy ICAT reagent-labeled BSA.

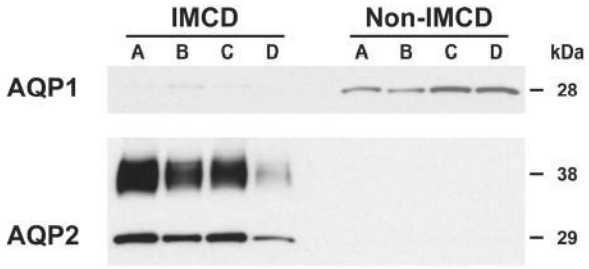

Figure 2.
Immunoblots demonstrating the quality of IMCD and non-IMCD samples preparation.

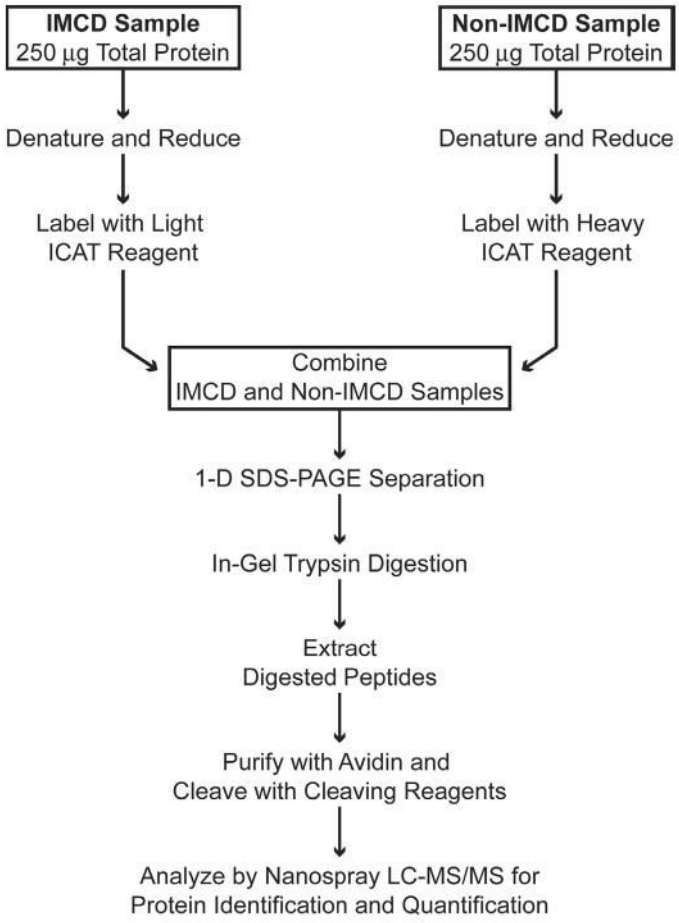

Figure 3.
Flow diagram of ICAT procedure in the IMCD vs. non-IMCD study.

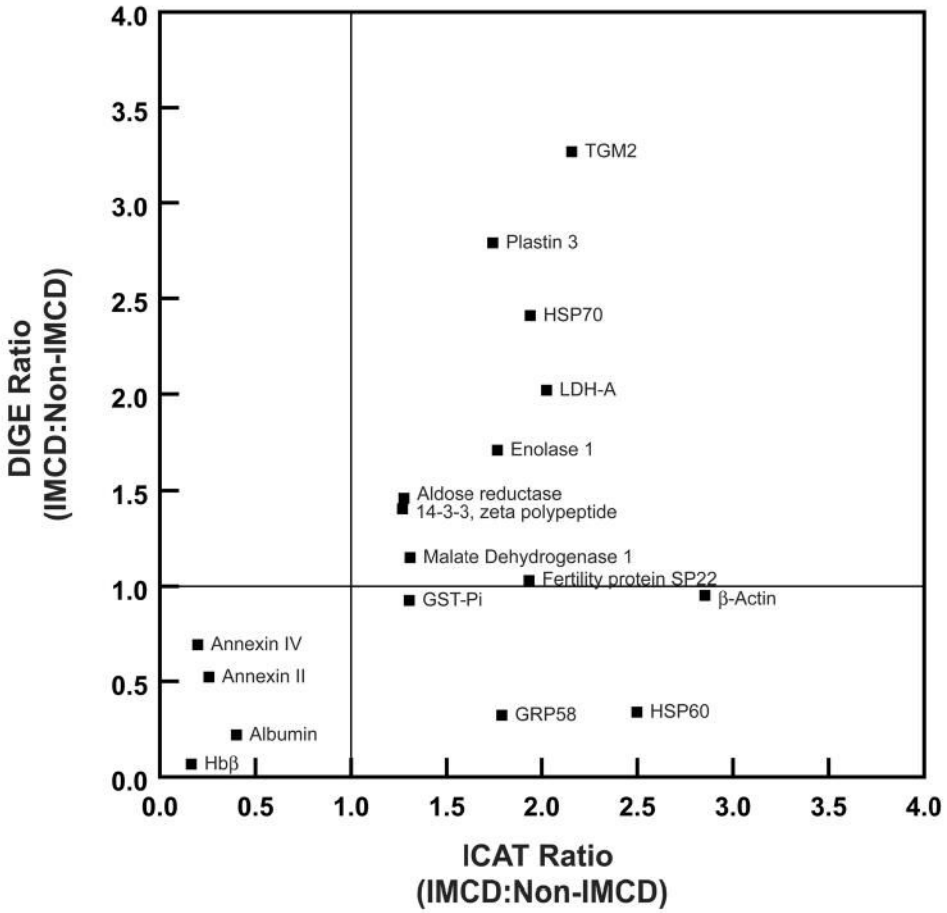

Figure 4.

Scatter graph illustrating correlation between ICAT and DIGE results of the IMCD vs. non-IMCD studies (n = 17, r = 0.45, p-value = 0.07). Abbreviations: GRP58 = glucose regulated protein, 58 kDa; GST-Pi = glutathione S-transferase, Pi; Hbβ = hemoglobin beta chain complex; HSP60 = heat shock 60kDa protein 1; HSP70 = heat shock 70kDa protein; LDH-A = lactate dehydrogenase A; TGM2 = transglutaminase 2.

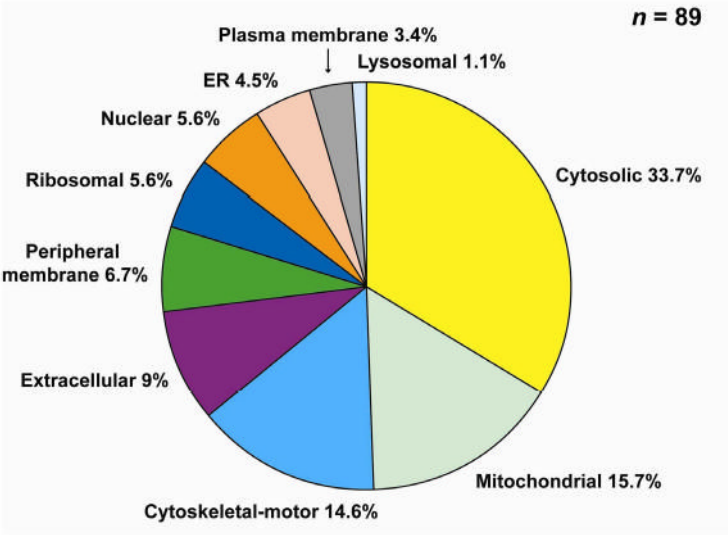

Figure 5.
Pie chart showing overall types of proteins identified in the IMCD vs. non-IMCD study.

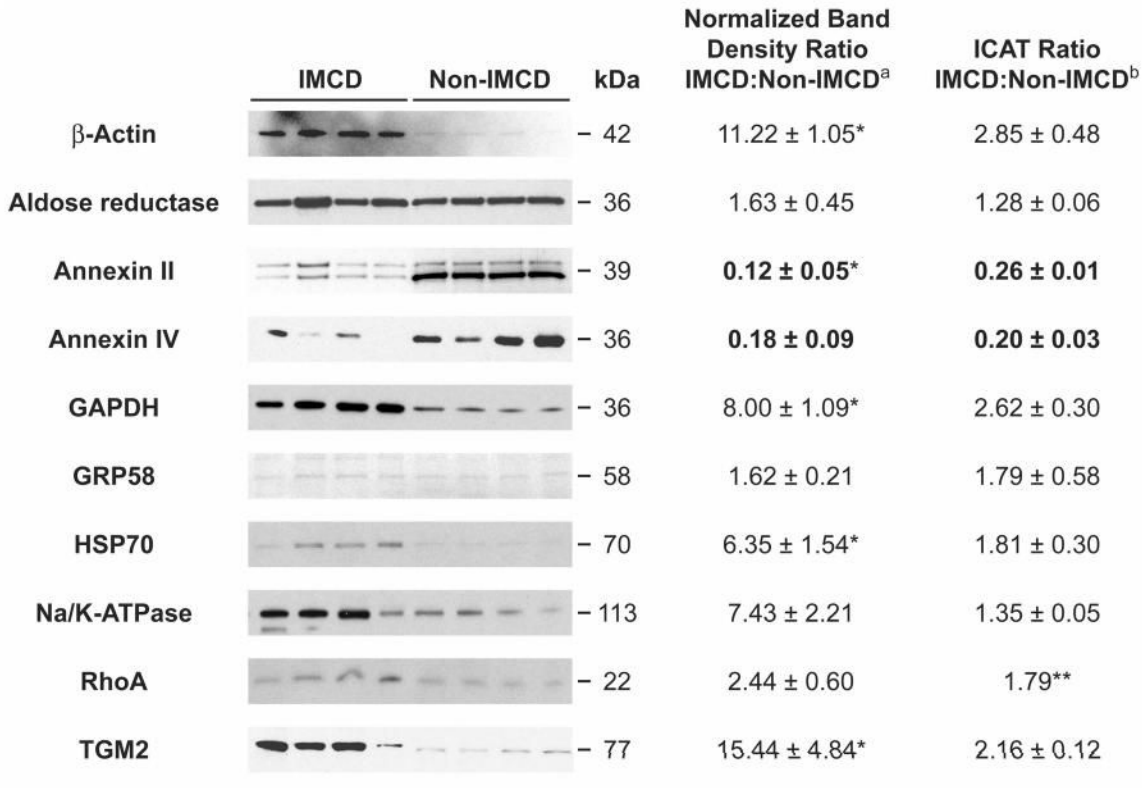

Figure 6.

Immunoblots confirmation of IMCD vs. non-IMCD ICAT results. a) mean ± SE; * significantly different (n = 8, 4 IMCD and 4 non-IMCD). b) mean ± SE; ** based on 1 ICAT ratio value. Regular font indicates ratio value more than 1 and bold font indicates ratio value less than 1. Abbreviations: GAPDH = glyceraldehyde-3-phosphate dehydrogenase; GRP58 = glucose regulated protein, 58 kDa; HSP70 = heat shock 70kDa protein; TGM2 = transglutaminase 2.

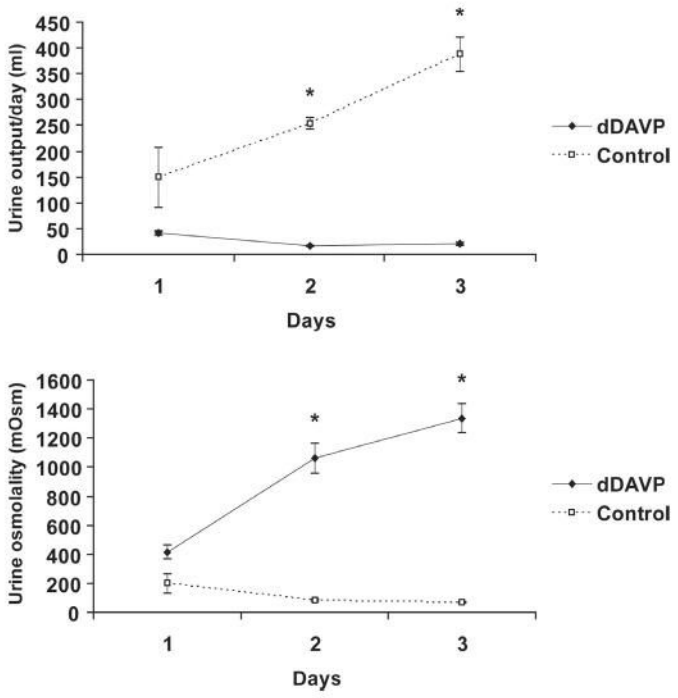

Figure 7.
Urine output and urine osmolality between the dDAVP and control groups. * significantly different from the control group, p-value < 0.05.

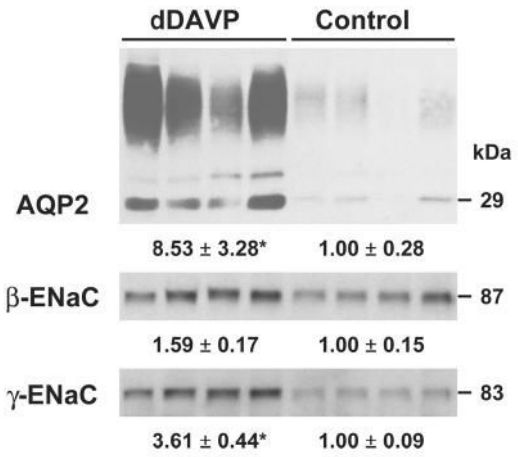

Figure 8.
Immunoblots of AQP2, β-ENaC, and γ-ENaC confirming the action of the infused dDAVP. Normalized band densities are shown as mean ± SE. * significantly different from the control group, p-value < 0.05.

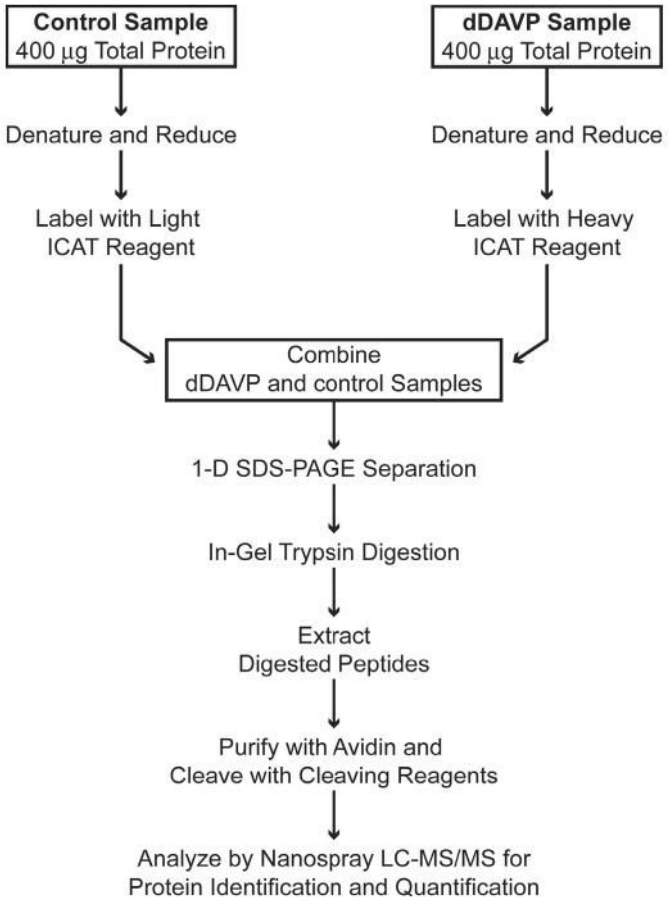

Figure 9.
Flow diagram of the ICAT analysis of response to long-term dDAVP administration in IMCD from Brattleboro rats.

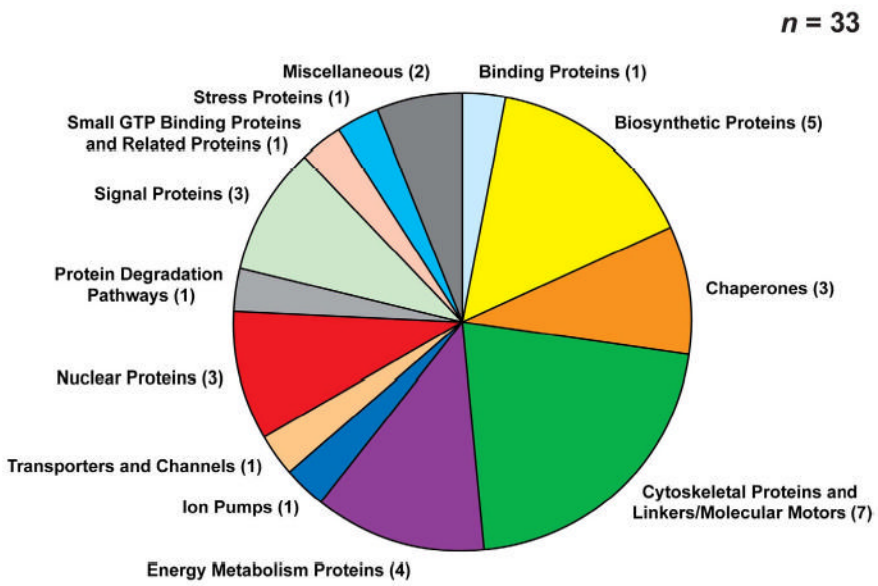

Figure 10.
Pie chart illustrating types of proteins that significantly changed in abundance as a result of long-term vasopressin action, a classification of these proteins is based on the Collecting Duct Database (CDDB) identifiers (24).

A.

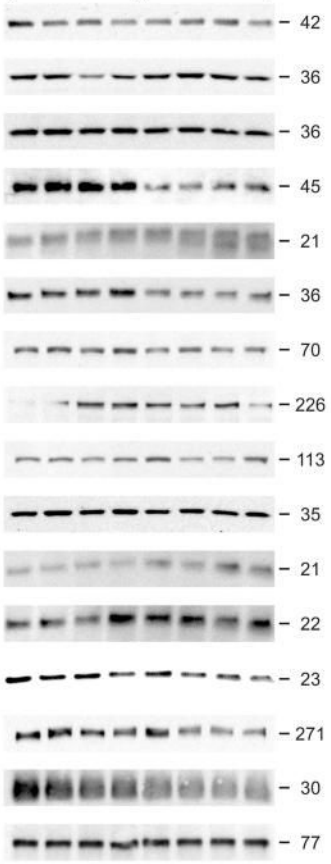

	dDAVP / Control	kDa	Normalized Band Density Ratio dDAVP:Control[a]	ICAT Ratio dDAVP:Control[b]	Number of Unique Peptides Identified by LC-MS/MS
β-Actin		42	1.11 ± 0.18	1.28 ± 0.06*	7
Aldose reductase		36	**0.77 ± 0.11**	**0.80 ± 0.02***	7
Annexin IV		36	1.30 ± 0.08	1.86 ± 0.93	6
Cathepsin D		45	3.18 ± 0.26*	1.78 ± 0.25*	2
Cdc42		21	**0.91 ± 0.07**	**0.92 ± 0.04**	4
GAPDH		36	1.66 ± 0.09*	1.33 ± 0.06*	5
HSP70		70	1.50 ± 0.13*	1.21 ± 0.06*	7
Myosin IIA		226	**0.93 ± 0.50**	**0.95 ± 0.04**	9
Na/K-ATPase		113	**0.91 ± 0.06**	**0.87 ± 0.04***	9
RACK1		35	1.35 ± 0.14	**0.49****	1
Rap1		21	**0.62 ± 0.05***	2.04**	1
RhoA		22	**0.96 ± 0.12**	**0.80 ± 0.07***	5
RhoGDI-1		23	1.18 ± 0.15	1.85**	1
β-Spectrin		271	2.24 ± 0.40	1.64 ± 0.07*	1
Syntaxin-7		30	1.92 ± 0.21*	1.27 ± 0.32	2
TGM2		77	1.21 ± 0.06	1.06 ± 0.20	5

B.

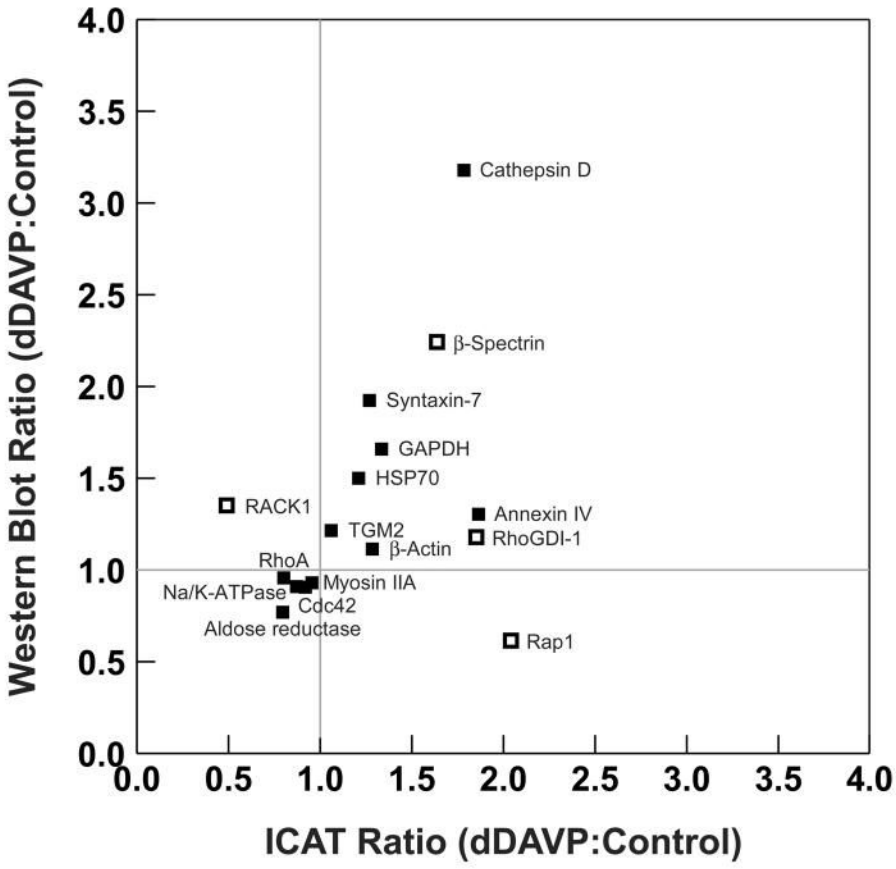

Figure 11.

A) Confirmatory immunoblots of the ICAT analysis of response to long-term dDAVP administration in IMCD from Brattleboro rats. a) mean ± SE; * significantly different (n = 8, 4 dDAVP and 4 control). b) mean ± SE; * significantly different from 1.00 based on observations in 3 or more quantifiable spectra; ** based on 1 ICAT ratio value. Regular font indicates ratio value more than 1 and bold font indicates ratio value less than 1. **B**) Scatter graph illustrating correlation between ICAT and western blot ratios (dDAVP:Control). Black boxes represent proteins identified from two or more unique peptides (n = 12) and white boxes represent proteins identified from one unique peptides (n = 4). Correlation between ICAT and western blot ratios was significant (r = 0.72) when proteins identified from two or more peptides were analyzed, however, the correlation was not significant (r = 0.34) when every proteins were analyzed. Abbreviations: GAPDH = glyceraldehyde-3-phosphate dehydrogenase; HSP70 = heat shock 70kDa protein; Myosin IIA = myosin heavy chain, nonmuscle IIA; RACK1 = receptor of activated protein kinase C 1; TGM2 = transglutaminase 2.

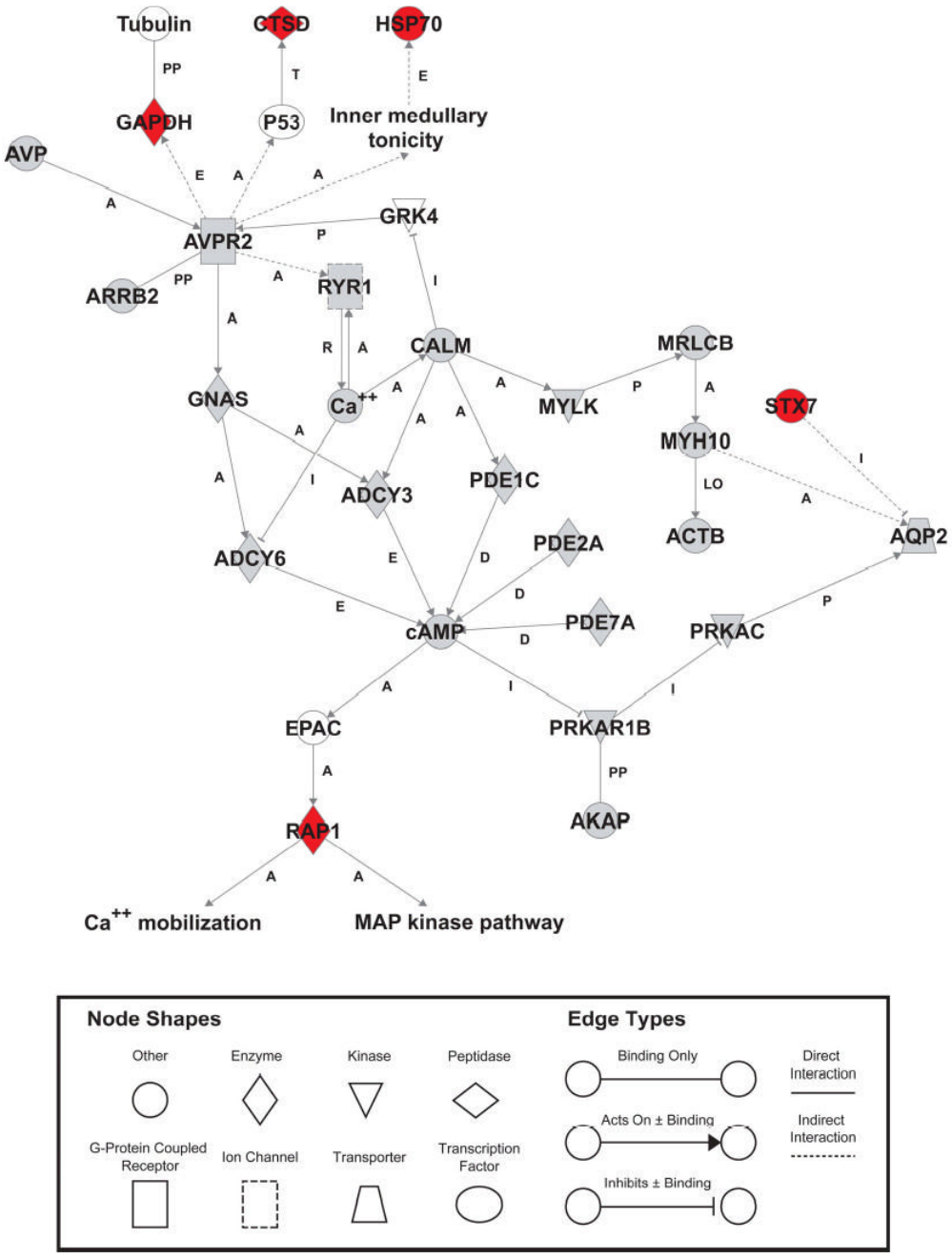

Figure 12.

Bioinformatic network representing the core signaling pathway downstream from V2R occupation in IMCD demonstrated by previous studies (labeled in grey) and the five proteins regulated in response to long-term dDAVP administration that were validated by immunoblotting in this study (labeled in red). Unfilled nodes (white background) represent IMCD proteins chosen to connect the core network with the red nodes. Supplementary Table 3 describes the interactions between parent nodes and child nodes in the bioinformatic network. Supplementary Table 4 demonstrates protein names and references documenting the presence of each protein in IMCD. Edge labels: A = Activation; D = Degradation; E = Expression; I =

Inhibition; LO = Translocation; P = Phosphorylation; PP = Protein-protein interaction; R = Release; and T = Transcription.

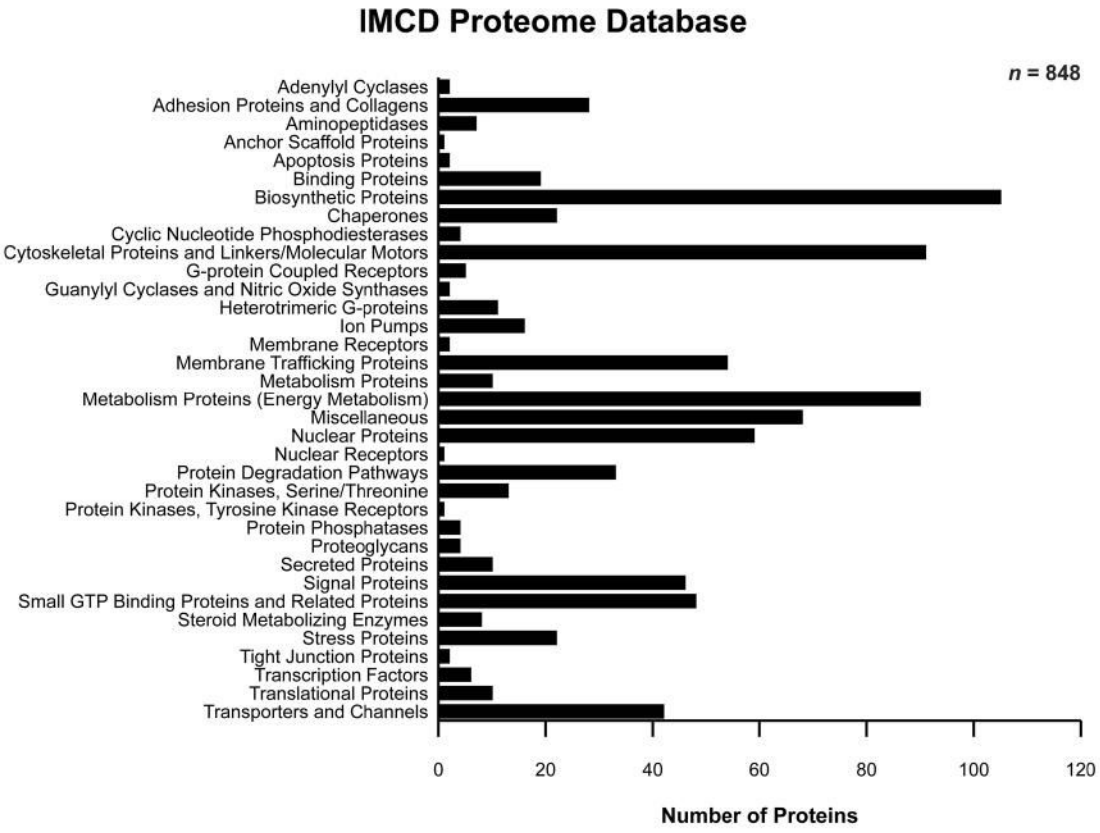

Figure 13.

Bar graph representing the distribution of 848 proteins in the IMCD Proteome Database categorized by the Collecting Duct Database (CDDB) identifiers (24).

Table 1

Proteins identified and quantification of protein abundances from IMCD vs. non-IMCD samples. Table reports only those proteins identified based on two or more unique tryptic peptides (n=44).

Protein Name	Accession Number	Unique Peptide Number (Quantifiable Spectra Number)	ICAT Ratio IMCD:Non-IMCD (Mean ± SE)	DIGE Ratio IMCD:Non-IMCD[a]
Pyruvate kinase 3	NP_445749	4 (11)	3.54 ± 0.56	
Beta-actin	NP_112406	4 (28)	2.85 ± 0.48	0.95
Glutathione S-transferase, Mu 1	NP_058710	4 (7)	2.73 ± 0.42	
Glyceraldehyde-3-phosphate dehydrogenase	NP_058704	4 (32)	2.62 ± 0.30	
Heat shock 60kDa protein 1 (chaperonin)	NP_071565	2 (3)	2.50 ± 1.07	0.34
Transglutaminase 2	NP_062259	2 (2)	2.16 ± 0.12	3.27
Similar to sid23p	XP_215862	3 (4)	2.12 ± 0.07	
High mobility group box 1	NP_037095	2 (6)	2.03 ± 0.46	
Lactate dehydrogenase A	NP_058721	3 (26)	2.03 ± 0.14	2.02
Glutathione S-transferase, Mu 2	NP_803175	5 (22)	1.99 ± 0.10	
Heat shock 70kDa protein 1A or 1B	1A:NP_114177 1B:NP_997669	3 (5)	1.94 ± 0.34	2.41
Fertility protein SP22	NP_476484	3 (5)	1.93 ± 0.27	1.03
Peptidylprolyl isomerase A	NP_058797	3 (7)	1.83 ± 0.09	
Calgizzarin	NP_001004095	2 (5)	1.82 ± 0.01	
Glucose regulated protein, 58 kDa	NP_059015	2 (7)	1.79 ± 0.58	0.32
Phosphoglycerate kinase 1	NP_445743	3 (3)	1.79 ± 0.33	
Enolase 1, alpha	NP_036686	2 (19)	1.77 ± 0.11	1.71
Filamin B	XP_127565	6 (10)	1.76 ± 0.11	
Plastin 3 (T-isoform)	XP_343777	2 (2)	1.74 ± 0.48	2.79
WD-repeat protein 1	NP_035845	2 (2)	1.71 ± 0.33	
Triosephosphate isomerase 1	NP_075211	7 (15)	1.49 ± 0.05	
60S ribosomal protein L12	NP_033102	4 (8)	1.39 ± 0.10	
ATPase, Na+K+ transporting, alpha 1 or alpha 2	1:NP_036636 2:NP_036637	6 (37)	1.35 ± 0.05	
Malate dehydrogenase 1	NP_150238	2 (6)	1.31 ± 0.02	1.15
Glutathione S-transferase, Pi or Pi 2	pi:NP_036709 pi 2:NP_620430	2 (2)	1.30 ± 0.08	0.93
Enolase 2, gamma	NP_647541	2 (3)	1.29 ± 0.12	
Aldose reductase	NP_036630	8 (92)	1.28 ± 0.06	1.46
14-3-3, zeta polypeptide	NP_037143	2 (10)	1.27 ± 0.03	1.41
Cdc42 or Rac1	Cdc42:NP_741991 Rac1:NP_599193	2 (7)	1.14 ± 0.13	
Mitochondrial ATP synthase, O subunit	NP_620238	2 (7)	0.88 ± 0.10	
Laminin gamma-1 chain	XP_341134	4 (4)	0.86 ± 0.14	
Cofilin 1	NP_058843	2 (9)	0.83 ± 0.15	
Tumor-associated calcium signal transducer 1	NP_612550	2 (2)	0.82 ± 0.05	
ATP synthase subunit D	NP_062256	2 (7)	0.75 ± 0.001	
Ubiquinol-cytochrome c reductase core protein I	NP_001004250	2 (2)	0.74 ± 0.01	
Isocitrate dehydrogenase [NADP], mitochondrial	NP_766599	3 (9)	0.62 ± 0.12	
Acidic ribosomal protein P0	NP_071797	2 (2)	0.60**	
Malate dehydrogenase 2	NP_112413	4 (13)	0.59 ± 0.05	
Laminin, beta 2	NP_037106	2 (3)	0.57 ± 0.17	
Ceruloplasmin	NP_036664	2 (2)	0.48 ± 0.11	
Albumin	NP_599153	10 (40)	0.40 ± 0.03	0.22
Annexin A2	NP_063970	5 (123)	0.26 ± 0.01	0.52
Annexin A4	NP_077069	3 (37)	0.20 ± 0.03	0.69
Hemoglobin beta chain complex	NP_150237	2 (7)	0.16 ± 0.02	0.07

** based on 1 ICAT ratio value.

[a] data from Hoffert et al (15).

Table 2

Proteins identified that were significantly increased or decreased in abundance (dDAVP:control ratios different from 1.00 based on observations in 3 or more quantifiable spectra) in response to long-term dDAVP administration in IMCD from Brattleboro rats (n = 33).

Protein Name	Accession Number	Unique Peptide Number (Quantifiable Spectra Number)	ICAT Ratio dDAVP:Control (Mean ± SE)
Cathepsin D	NP_599161	2 (8)	1.78 ± 0.25
Beta-spectrin 3	NP_062040	1 (3)	1.64 ± 0.07
Heat-shock protein 105 kDa	NP_001011901	4 (5)	1.58 ± 0.12
Protein kinase C, iota	NP_071528	2 (4)	1.56 ± 0.08
Albumin	NP_599153	13 (15)	1.54 ± 0.19
Capping protein (actin filament), gelsolin-like	NP_001013104	2 (4)	1.53 ± 0.01
Creatine kinase	NP_036661	2 (9)	1.34 ± 0.07
Glyceraldehyde-3-phosphate dehydrogenase	NP_058704	5 (60)	1.33 ± 0.06
Heat shock 70kDa protein 8	NP_077327	2 (4)	1.33 ± 0.05
Beta-actin	NP_112406	7 (88)	1.28 ± 0.06
Filamin A	XP_238167	5 (8)	1.24 ± 0.09
Plastin 3 (T-isoform)	XP_343777	2 (4)	1.24 ± 0.02
Enolase 1, alpha	NP_036686	6 (22)	1.22 ± 0.07
Tubulin, beta 5	NP_775125	4 (13)	1.19 ± 0.06
Heat shock 70kDa protein 1A or 1B	1A:NP_114177 1B:NP_997669	5 (17)	1.18 ± 0.07
High mobility group box 1	NP_037095	2 (11)	1.15 ± 0.01
60S ribosomal protein L12	XP_216039	4 (4)	1.14 ± 0.02
Ribosomal protein L23	NP_001007600	2 (4)	1.12 ± 0.02
Peptidylprolyl isomerase A	NP_058797	7 (21)	1.11 ± 0.03
Triosephosphate isomerase 1	NP_075211	12 (46)	1.11 ± 0.04
14-3-3, zeta polypeptide	NP_037143	2 (16)	1.10 ± 0.03
Lactate dehydrogenase B	NP_036727	3 (39)	1.07 ± 0.03
Voltage-dependent anion channel 1	NP_112643	2 (3)	0.90 ± 0.003
H3 histone, family 3B	NP_446437	2 (30)	0.88 ± 0.05
ATPase, Na+K+ transporting, alpha 1	NP_036636	9 (28)	0.87 ± 0.04
S100 calcium binding protein A11	NP_001004095	2 (59)	0.85 ± 0.07
Myosin heavy chain, nonmuscle IIB	NP_113708	4 (8)	0.83 ± 0.06
Ras homolog gene family, member A	NP_476473	5 (8)	0.80 ± 0.07
Aldose reductase	NP_036630	7 (65)	0.80 ± 0.02
Ribosomal protein S3	NP_001009239	2 (4)	0.75 ± 0.04
Similar to Transmembrane protein 16F	XP_235640	2 (3)	0.75 ± 0.02
Acid nuclear phosphoprotein 32 (leucine rich)	NP_037035	2 (3)	0.74 ± 0.03
Similar to LBA	XP_342272	7 (12)	0.70 ± 0.11

Supplementary Table 1

Full results for all proteins identified from the IMCD vs. non-IMCD ICAT study (n = 89).

Protein Name	Accession Number	Unique Peptide Number (Quantifiable Spectra Number)	ICAT Ratio IMCD:Non-IMCD (Mean ± SE)	DIGE Ratio IMCD:Non-IMCD[a]
Actin-like protein 2	P61161	1 (1)	7.69**	
Tubulin, beta 3 or beta 4 or beta 5	3:NP_640347 4:Q9D6F9 5:NP_775125	1 (5)	6.35 ± 1.12	1.16
Clathrin, heavy polypeptide (Hc)	NP_062172	1 (1)	4.35**	
Actin-related protein 3 homolog	XP_341113	1 (1)	4.17**	
Pyruvate kinase 3	NP_445749	4 (11)	3.54 ± 0.56	
Beta-actin	NP_112406	4 (28)	2.85 ± 0.48	0.95
Glutathione S-transferase, Mu 1	NP_058710	4 (7)	2.73 ± 0.42	
Heterogeneous nuclear ribonucleoprotein A1	NP_058944	1 (1)	2.63**	
Glyceraldehyde-3-phosphate dehydrogenase	NP_058704	4 (32)	2.62 ± 0.30	
Heat shock 60kDa protein 1 (chaperonin)	NP_071565	2 (3)	2.50 ± 1.07	0.34
Dithiolethione-inducible gene-1	NP_620218	1 (3)	2.50 ± 0.21	
Transgelin 2	Q9WVA4	1 (3)	2.40 ± 0.16	
Actinin, alpha 1 or alpha 3 or alpha 4	1:NP_112267 3:NP_596915 4:NP_113863	1 (1)	2.27**	
14-3-3, theta polypeptide	NP_037185	1 (1)	2.22**	
40S ribosomal protein S12	P09388	1 (2)	2.21 ± 0.82	
Heat-shock protein 105 kDa	Q61699	1 (1)	2.17**	
Transglutaminase 2	NP_062259	2 (2)	2.16 ± 0.12	3.27
Carboxylesterase 2	NP_598270	1 (1)	2.13**	
Similar to sid23p	XP_215862	3 (4)	2.12 ± 0.07	
Aldolase A	NP_036627	1 (2)	2.07 ± 0.15	1.37
Glutamate dehydrogenase 1	NP_036702	1 (1)	2.04**	0.26
Macrophage migration inhibitory factor	NP_112313	1 (2)	2.04**	
High mobility group box 1	NP_037095	2 (6)	2.03 ± 0.46	
Lactate dehydrogenase A	NP_058721	3 (26)	2.03 ± 0.14	2.02
Glutathione S-transferase, Mu 2	NP_803175	5 (22)	1.99 ± 0.10	
ATP synthase, H+ transporting, mitochondrial F1 complex, gamma subunit	NP_446277	1 (1)	1.96**	
Heat shock 70kDa protein 1A or 1B	1A:NP_114177 1B:NP_997669	3 (5)	1.94 ± 0.34	2.41
Fertility protein SP22	NP_476484	3 (5)	1.93 ± 0.27	1.03
Peptidylprolyl isomerase A	NP_058797	3 (7)	1.83 ± 0.09	
Calgizzarin	NP_001004095	2 (5)	1.82 ± 0.01	
Phosphoglycerate mutase 1	NP_445742	1 (1)	1.82**	
Glucose regulated protein, 58 kDa	NP_059015	2 (7)	1.79 ± 0.58	0.32
Phosphoglycerate kinase 1	NP_445743	3 (3)	1.79 ± 0.33	
Ras homolog gene family, member A	NP_476473	1 (1)	1.79**	
Ribosomal protein L23	XP_213448	1 (1)	1.79**	
Enolase 1, alpha	NP_036686	2 (19)	1.77 ± 0.11	1.71
Filamin B	XP_127565	6 (10)	1.76 ± 0.11	
Carbonic anhydrase 2	NP_062164	1 (2)	1.76 ± 0.24	1.25
Protein kinase C, iota	NP_071528	1 (1)	1.75**	
Plastin 3 (T-isoform)	XP_343777	2 (2)	1.74 ± 0.48	2.79
Cysteine and glycine-rich protein 1	NP_058844	1 (1)	1.72**	
Fibrillin-1	NP_114013	1 (1)	1.72**	
Eukaryotic translation elongation factor 2	NP_058941	1 (3)	1.72 ± 0.27	
Wd-repeat protein 1	NP_035845	2 (2)	1.71 ± 0.33	
Coiled-coil-helix-coiled-coil-helix domain containing 3	NP_079612	1 (1)	1.69**	
Cathepsin D	NP_599161	1 (1)	1.52**	
Triosephosphate isomerase 1	NP_075211	7 (15)	1.49 ± 0.05	
RNA polymerase II elongation factor ELL	O08856	1 (1)	1.47**	
Tropomyosin isoform 6	NP_775134	1 (1)	1.45**	
Chloride intracellular channel 1	NP_001002807	1 (1)	1.43**	
60S ribosomal protein L12	NP_033102	4 (8)	1.39 ± 0.10	
Thioredoxin domain containing protein 4	Q9D1Q6	1 (1)	1.39**	
ATPase, Na+K+ transporting, alpha 1 or alpha 2	1:NP_036636 2:NP_036637	6 (37)	1.35 ± 0.05	
14-3-3, gamma polypeptide	NP_062249	1 (1)	1.32**	
Malate dehydrogenase 1	NP_150238	2 (6)	1.31 ± 0.02	1.15
Glutathione S-transferase, Pi or Pi 2	pi:NP_036709 pi 2:NP_620430	2 (2)	1.30 ± 0.08	0.93

Protein Name	Accession Number	Unique Peptide Number (Quantifiable Spectra Number)	ICAT Ratio IMCD:Non-IMCD (Mean ± SE)	DIGE Ratio IMCD:Non-IMCD[a]
Enolase 2, gamma	NP_647541	2 (3)	1.29 ± 0.12	
Aldose reductase	NP_036630	8 (92)	1.28 ± 0.06	1.46
14-3-3, zeta polypeptide	NP_037143	2 (10)	1.27 ± 0.03	1.41
Mitochondrial H+-ATP synthase alpha subunit	NP_075581	1 (1)	1.20**	0.33
Heat shock 70kDa protein 8	NP_077327	1 (1)	1.18**	1.28
Cdc42 or Rac1	Cdc42:NP_741991 Rac1:NP_599193	2 (7)	1.14 ± 0.13	
ATPase Na+/K+ transporting beta 1 polypeptide	NP_037245	1 (3)	1.09 ± 0.18	
Calreticulin	NP_071794	1 (1)	1.01**	0.34
Fatty acid binding protein 5, epidermal	NP_665885	1 (1)	1.00**	
Ribosomal protein S17	NP_058848	1 (1)	0.97**	
NAD(P) transhydrogenase, mitochondrial	Q61941	1 (1)	0.96**	
Mitochondrial ATP synthase, O subunit	NP_620238	2 (7)	0.88 ± 0.10	
Laminin gamma-1 chain	XP_341134	4 (4)	0.86 ± 0.14	
Laminin, alpha 5	XP_215963	1 (1)	0.84**	
Cofilin 1	NP_058843	2 (9)	0.83 ± 0.15	
Tumor-associated calcium signal transducer 1	NP_612550	2 (2)	0.82 ± 0.05	
ATP synthase subunit D	NP_062256	2 (7)	0.75 ± 0.00	
Ubiquinol-cytochrome c reductase core protein I	NP_001004250	2 (2)	0.74 ± 0.01	
Glutamate oxaloacetate transaminase 2	NP_037309	1 (3)	0.70 ± 0.20	0.24
Solute carrier family 25, member 4 or member 5	4:NP_445967 5:NP_476443	1 (3)	0.65 ± 0.19	
Voltage-dependent anion channel 1	NP_112643	1 (1)	0.63**	0.26
Isocitrate dehydrogenase [NADP], mitochondrial	NP_766599	3 (9)	0.62 ± 0.12	
Acidic ribosomal protein P0	NP_071797	2 (2)	0.60**	
Malate dehydrogenase 2	NP_112413	4 (13)	0.59 ± 0.05	
Laminin, beta 2	NP_037106	2 (3)	0.57 ± 0.17	
Ceruloplasmin	NP_036664	2 (2)	0.48 ± 0.11	
Serotransferrin	P12346	1 (1)	0.43**	
Albumin	NP_599153	10 (40)	0.40 ± 0.03	0.22
Annexin A11	P97384	1 (1)	0.32**	
Annexin A2	NP_063970	5 (123)	0.26 ± 0.01	0.52
Annexin A4	NP_077069	3 (37)	0.20 ± 0.03	0.69
Hemoglobin beta chain complex	NP_150237	2 (7)	0.16 ± 0.02	0.07
Zinc finger protein 161	NP_758828	1 (1)	0.03**	

** based on 1 ICAT ratio value.

[a] data from Hoffert et al (15).

Supplementary Table 2

Full results for all proteins identified from the ICAT analysis of response to long-term dDAVP administration in IMCD from Brattleboro rats (n = 165).

Protein Name	Accession Number	Unique Peptide Number (Quantifiable Spectra Number)	ICAT Ratio dDAVP:Control (Mean ± SE)
Ribosomal protein L30	NP_073190	2 (5)	2.78**
Metallothionein-II	P04355	1 (2)	2.70**
Rab3D	NP_542147	1 (1)	2.04**
Rap1B	NP_599173	1 (1)	2.04**
Rap1A	NP_001005765	1 (1)	2.04**
Diacetyl/L-xylulose reductase	NP_599214	1 (1)	1.96**
Solute carrier family 25 (mitochondrial carrier; phosphate carrier), member 3	NP_620800	1 (1)	1.96**
Annexin A4	NP_077069	6 (17)	1.86 ± 0.93
RhoGDI-1	NP_001007006	1 (1)	1.85**
Cathepsin D	NP_599161	2 (8)	1.78 ± 0.25*
F-actin capping protein beta subunit	NP_001005903	1 (1)	1.75**
Similar to WD-repeat protein 1	XP_341230	1 (1)	1.69**
Ubiquinol-cytochrome c reductase core protein I	NP_001004250	2 (2)	1.64 ± 0.17
Beta-spectrin 3	NP_062040	1 (3)	1.64 ± 0.07*
Similar to sid23p	XP_215862	6 (10)	1.63 ± 0.36
Heat-shock protein 105 kDa	NP_001011901	4 (5)	1.58 ± 0.12*
Protein kinase C, iota	NP_071528	2 (4)	1.56 ± 0.08*
Ubiquitin carboxy-terminal hydrolase L1	NP_058933	2 (3)	1.54 ± 0.34
Albumin	NP_599153	13 (15)	1.54 ± 0.19*
40S ribosomal protein S17	XP_346082	2 (2)	1.53 ± 0.03
Capping protein (actin filament), gelsolin-like	NP_001013104	2 (4)	1.53 ± 0.01*
Calpain, small subunit 1	XP_341825	1 (1)	1.52**
Catenin (cadherin-associated protein), alpha 1, 102kDa	NP_001007146	2 (4)	1.50 ± 0.25
Valosin-containing protein	NP_446316	3 (4)	1.48 ± 0.38
S-adenosylhomocysteine hydrolase	NP_058897	1 (1)	1.47**
Similar to headcase homolog; hHDC for homolog of Drosophila headcase	XP_218660	1 (1)	1.45**
Similar to periplakin	XP_220174	2 (3)	1.43 ± 0.36
Dynein, cytoplasmic, heavy chain 1	NP_062099	1 (1)	1.37**
Similar to Bifunctional aminoacyl-tRNA synthetase	XP_213969	1 (1)	1.37**
Malate dehydrogenase 1, NAD (soluble)	NP_150238	3 (5)	1.36 ± 0.26
Lutheran blood group (Auberger b antigen included)	NP_113940	2 (2)	1.35 ± 0.40
Calreticulin	NP_071794	1 (1)	1.35**
Creatine kinase	NP_036661	2 (9)	1.34 ± 0.07*
Glyceraldehyde-3-phosphate dehydrogenase	NP_058704	5 (60)	1.33 ± 0.06*
Gelsolin	NP_001004080	1 (1)	1.33**
Heat shock 70kDa protein 8	NP_077327	2 (4)	1.33 ± 0.05*
Methylmalonate semialdehyde dehydrogenase gene	NP_112319	1 (1)	1.32**
Beta-actin	NP_112406	7 (88)	1.28 ± 0.06*
Beta-galactoside-binding lectin	NP_063969	1 (1)	1.28**
Syntaxin-7	NP_068641	2 (2)	1.27 ± 0.32
14-3-3, epsilon polypeptide	NP_113791	2 (2)	1.27 ± 0.02
Filamin A	XP_238167	5 (8)	1.24 ± 0.09*
Telomerase-binding protein p23	NP_062740	2 (2)	1.24 ± 0.21
Plastin 3 (T-isoform)	XP_343777	2 (4)	1.24 ± 0.02*
Transgelin 2	NP_001013145	1 (1)	1.23**
Aldehyde dehydrogenase family 1, member A1	NP_071852	1 (1)	1.22**
Enolase 1, alpha	NP_036686	6 (22)	1.22 ± 0.07*
Similar to laminin gamma-1 chain precursor	XP_341134	4 (4)	1.22 ± 0.10
Tubulin, beta 5	NP_775125	4 (13)	1.19 ± 0.06*
Heat shock 70kDa protein 1A or 1B	1A:NP_114177 1B:NP_997669	5 (17)	1.18 ± 0.07*
Alpha-ETF	NP_001009668	2 (2)	1.18**
Eukaryotic translation elongation factor 1 alpha 2	NP_284925	2 (4)	1.17 ± 0.11
Eukaryotic translation elongation factor 1 alpha 1	NP_787032	2 (4)	1.17 ± 0.11
Ubiquitin-conjugating enzyme E2D 3	NP_112516	1 (1)	1.16**
Annexin 1	NP_037036	2 (10)	1.16 ± 0.14
Myosin light polypeptide 6	XP_222163	1 (1)	1.15**
High mobility group box 1	NP_037095	2 (11)	1.15 ± 0.01*
60S ribosomal protein L12	XP_216039	4 (4)	1.14 ± 0.02*
Ribosomal protein L23	NP_001007600	2 (4)	1.12 ± 0.02*

Protein Name	Accession Number	Unique Peptide Number (Quantifiable Spectra Number)	ICAT Ratio dDAVP:Control (Mean ± SE)
Fibrillin-1	NP_114013	4 (4)	1.12 ± 0.13
Peroxiredoxin 5 precursor	NP_446062	3 (9)	1.11 ± 0.13
Glutathione S-transferase, Mu 1	NP_058710	7 (14)	1.11 ± 0.04
Heat shock protein 1, alpha	NP_786937	1 (1)	1.11**
Peptidylprolyl isomerase A	NP_058797	7 (21)	1.11 ± 0.03*
Triosephosphate isomerase 1	NP_075211	12 (46)	1.11 ± 0.04*
Isocitrate dehydrogenase 2 (NADP+), mitochondrial	NP_766599	3 (4)	1.10 ± 0.23
14-3-3, zeta polypeptide	NP_037143	2 (16)	1.10 ± 0.03*
Laminin, beta 2	NP_037106	1 (1)	1.10**
Latexin	NP_113843	1 (1)	1.10**
Glutathione S-transferase, Pi	NP_036709	2 (2)	1.09 ± 0.01
Glutathione S-transferase, Pi 2	NP_620430	2 (2)	1.09 ± 0.01
Ribosomal protein L9	NP_001007599	2 (5)	1.09 ± 0.01
Acidic ribosomal protein P0	NP_071797	3 (6)	1.09 ± 0.11
Ubiquitin specific protease 14	NP_001008302	2 (3)	1.08 ± 0.20
Glucose regulated protein, 58 kDa	NP_059015	2 (19)	1.08 ± 0.05
Tropomyosin isoform 6	NP_775134	1 (1)	1.08**
Lactate dehydrogenase B	NP_036727	3 (39)	1.07 ± 0.03*
Glutamate oxaloacetate transaminase 2	NP_037309	3 (4)	1.07 ± 0.24
Mitochondrial ATP synthase, O subunit	NP_620238	2 (7)	1.06 ± 0.03
Transglutaminase 2	NP_062259	5 (10)	1.06 ± 0.20
Agrin	NP_786930	3 (4)	1.06 ± 0.24
Hypoxanthine guanine phosphoribosyl transferase	NP_036715	1 (1)	1.05**
14-3-3, theta polypeptide	NP_037185	6 (20)	1.05 ± 0.04
60S ribosomal protein L18a	NP_997675	2 (2)	1.04 ± 0.13
Similar to Filamin B	XP_224561	11 (33)	1.04 ± 0.05
Lactate dehydrogenase A	NP_058721	4 (51)	1.04 ± 0.03
Actin-related protein 3 homolog	XP_341113	3 (5)	1.04 ± 0.13
Transaldolase 1	NP_113999	1 (1)	1.03**
Annexin A2	NP_063970	4 (40)	1.03 ± 0.08
M2 pyruvate kinase	NP_445749	9 (53)	1.02 ± 0.05
Similar to alpha-3 type IV collagen	XP_343608	1 (1)	1.02**
Glutathione S-transferase, Mu 3	NP_112416	5 (14)	1.02 ± 0.05
Phosphoglycerate mutase 1	NP_445742	2 (3)	1.02 ± 0.08
Glutathione S-transferase, Mu 2	NP_803175	8 (26)	1.02 ± 0.02
Macrophage migration inhibitory factor	NP_112313	2 (4)	1.01 ± 0.04
Aldolase A	NP_036627	3 (5)	1.00 ± 0.06
Ribosomal protein L13A	NP_775462	2 (3)	1.00 ± 0.31
Eukaryotic translation elongation factor 2	NP_058941	5 (7)	0.99 ± 0.11
Phosphoglycerate kinase 1	NP_445743	3 (8)	0.99 ± 0.15
Solute carrier family 25, member 4	NP_445967	2 (6)	0.99 ± 0.09
Solute carrier family 25, member 5	NP_476443	2 (6)	0.99 ± 0.09
ATPase Na+/K+ transporting beta 1 polypeptide	NP_037245	2 (7)	0.99 ± 0.10
Brain glycogen phosphorylase	XP_342543	2 (2)	0.99 ± 0.36
ATP synthase subunit D	NP_062256	2 (7)	0.98 ± 0.09
CAP, adenylate cyclase-associated protein 1	NP_071778	2 (2)	0.97**
Cysteine and glycine-rich protein 1	NP_058844	4 (5)	0.96 ± 0.03
Similar to IQ motif containing GTPase activating protein 1	XP_341878	1 (1)	0.96**
Rac1	NP_599193	4 (13)	0.96 ± 0.04
Actinin alpha 4	NP_113863	5 (13)	0.96 ± 0.06
Hydroxysteroid (17-beta) dehydrogenase 10	NP_113870	2 (3)	0.96 ± 0.22
Myosin heavy chain, nonmuscle IIA	NP_037326	9 (19)	0.95 ± 0.04
Heat shock 60kDa protein 1 (chaperonin)	NP_071565	2 (3)	0.93 ± 0.04
Aldehyde dehydrogenase family 1, subfamily A3	NP_695212	5 (16)	0.93 ± 0.08
Clathrin, heavy polypeptide (Hc)	NP_062172	13 (21)	0.92 ± 0.07
Similar to vacuolar protein sorting 13D isoform 1	XP_233792	1 (1)	0.92**
Cdc42	NP_741991	4 (12)	0.92 ± 0.04
Similar to actin related protein 2/3 complex, subunit 4	XP_238365	2 (3)	0.91 ± 0.09
Voltage-dependent anion channel 1	NP_112643	2 (3)	0.90 ± 0.003*
Similar to 40S ribosomal protein S11	XP_344733	1 (1)	0.90**
Similar to ribosomal protein S12	XP_344866	2 (2)	0.90 ± 0.06
Cofilin 1	NP_058843	3 (10)	0.89 ± 0.08
Ras homolog gene family, member Q	NP_445974	1 (1)	0.88**
H3 histone, family 3B	NP_446437	2 (30)	0.88 ± 0.05*
ATPase, Na+K+ transporting, alpha 1	NP_036636	9 (28)	0.87 ± 0.04*
Transferrin	NP_058751	1 (1)	0.87**
D-dopachrome tautomerase	NP_077045	3 (4)	0.87 ± 0.10
Similar to anti-A/dT antibody	XP_345730	2 (2)	0.87 ± 0.01

Protein Name	Accession Number	Unique Peptide Number (Quantifiable Spectra Number)	ICAT Ratio dDAVP:Control (Mean ± SE)
S100 calcium binding protein A11	NP_001004095	2 (59)	0.85 ± 0.07*
Similar to apoA-I binding protein	XP_215635	1 (1)	0.85**
Chloride intracellular channel 1	NP_001002807	1 (1)	0.84**
Fertility protein SP22	NP_476484	4 (5)	0.84 ± 0.11
Myosin heavy chain, nonmuscle IIB	NP_113708	4 (8)	0.83 ± 0.06*
Ras homolog gene family, member A	NP_476473	5 (8)	0.80 ± 0.07*
ATPase, Ca++ transporting, ubiquitous	NP_037046	1 (1)	0.80**
Abelson helper integration site 1	NP_001002277	1 (1)	0.80**
Similar to hypothetical protein 4833421E05Rik	XP_216665	1 (1)	0.80**
Aldose reductase	NP_036630	7 (65)	0.80 ± 0.02*
Malate dehydrogenase, mitochondrial	NP_112413	4 (6)	0.79 ± 0.06
Mitogen-activated protein kinase kinase kinase 8	NP_446299	1 (1)	0.78**
Similar to vacuolar protein sorting 29 isoform 2	XP_213780	1 (1)	0.78**
Similar to arginine/serine-rich 14 splicing factor	XP_341414	1 (1)	0.78**
CD59 antigen	NP_037057	2 (2)	0.77 ± 0.20
Similar to esterase D/formylglutathione hydrolase	XP_214241	1 (1)	0.76**
Ribosomal protein S3	NP_001009239	2 (4)	0.75 ± 0.04*
Similar to Transmembrane protein 16F	XP_235640	2 (3)	0.75 ± 0.02*
Acid nuclear phosphoprotein 32 (leucine rich)	NP_037035	2 (3)	0.74 ± 0.03*
RAN	NP_445891	2 (2)	0.74 ± 0.01
Microsomal signal peptidase 25 kDa subunit	XP_214994	1 (2)	0.73 ± 0.08
Similar to LBA	XP_342272	7 (12)	0.70 ± 0.11*
Plectin	NP_071796	2 (2)	0.70 ± 0.03
Leukotriene B4 12-hydroxydehydrogenase	NP_620218	1 (2)	0.70 ± 0.04
Transketolase	NP_072114	1 (2)	0.69 ± 0.01
H3 histone, family 2	XP_227460	1 (1)	0.64**
Utrophin	NP_037202	2 (2)	0.62 ± 0.03
Similar to Small nuclear ribonucleoprotein Sm D2	XP_214847	1 (1)	0.61**
Fatty acid binding protein 5, epidermal	NP_665885	1 (1)	0.60**
Similar to 0610010K06Rik protein	XP_223020	1 (2)	0.57**
Glutamate dehydrogenase 1	NP_036702	2 (2)	0.55 ± 0.07
Catechol-O-methyltransferase	NP_036663	1 (1)	0.52**
Tumor-associated calcium signal transducer 1	NP_612550	1 (1)	0.52**
RACK1	NP_570090	1 (1)	0.49**
Nidogen	XP_213954	1 (1)	0.49**
Similar to LY6/PLAUR domain containing 2	XP_216960	1 (2)	0.47 ± 0.18
Peptidase D	NP_001009641	1 (1)	0.39**
Similar to UDP-N-acteylglucosamine pyrophosphorylase 1	XP_216004	1 (1)	0.28**

* significantly different from 1.00 based on observations in 3 or more quantifiable spectra, p-value < 0.05.

** based on 1 ICAT ratio value.

Supplementary Table 3

The interactions between parent nodes and child nodes in the bioinformatic network (Figure 12). See Supplementary Table 4 for protein names and references.

Parent Node	Interaction	Child Node
ADCY3	directly catalyzes the formation of	cAMP
ADCY6	directly catalyzes the formation of	cAMP
AKAP	directly interacts with	PRKAR1B
AVP	directly activates	AVPR2
AVPR2	directly interacts with	ARRB2
AVPR2	directly activates	GNAS
AVPR2	indirectly activates	P53
AVPR2	indirectly activates	RYR1
AVPR2	indirectly increases the abundance of	GAPDH
AVPR2	indirectly increases	Inner medullary tonicity
Ca^{++}	directly inhibits	ADCY6
Ca^{++}	directly activates	CALM
Ca^{++}	directly activates	RYR1
CALM	directly activates	ADCY3
CALM	directly inhibits	GRK4
CALM	directly activates	MYLK
CALM	directly activates	PDE1C
cAMP	directly activates	EPAC
cAMP	directly inhibits	PRKAR1B
EPAC	directly activates	RAP1
GAPDH	directly interacts with	Tubulin
GNAS	directly activates	ADCY3
GNAS	directly activates	ADCY6
GRK4	directly phosphorylates	AVPR2
Inner medullary tonicity	indirectly affects the abundance of	HSP70
MRLCB	directly activates	MYH10
MYH10	directly affects the translocation of	ACTB
MYH10	indirectly activates the trafficking of	AQP2
MYLK	directly phosphorylates	MRLCB
P53	directly activates the transcriptional regulation of	CTSD
PDE1C	directly degrades	cAMP
PDE2A	directly degrades	cAMP
PDE7A	directly degrades	cAMP
PRKAC	directly phosphorylates	AQP2
PRKAR1B	directly inhibits	PRKAC
RAP1	directly activates	Ca^{++} mobilization
RAP1	directly activates	MAP kinase pathway
RYR1	directly releases	Ca^{++}
STX7	indirectly inhibits the apical expression of	AQP2

Supplementary Table 4

Protein names and references documenting the presence of each protein in IMCD for the bioinformatic network shown in Figure 12.

Node Name	Protein Name	References
ACTB	Beta-actin	*1*
ADCY3	Adenylate cyclase 3	*2*
ADCY6	Adenylate cyclase 6	*3*
AKAP	A-kinase anchor protein	*14*
AQP2	Aquaporin 2	*4*, *5*
ARRB2	Arrestin, beta 2	*6*
AVP	Arginine vasopressin	
AVPR2	Arginine vasopressin receptor 2	*7*
CALM	Calmodulin	*1*
CTSD	Cathepsin D	*1*
EPAC	Exchange factor directly activated by cAMP	*1*
GAPDH	Glyceraldehyde-3-phosphate dehydrogenase	*1*
GNAS	Guanine nucleotide-binding protein G(s), alpha subunit	*8*
GRK4	G protein-coupled receptor kinase 4	*9*
HSP70	Heat shock 70kDa protein	*1*
MRLCB	Myosin light chain, regulatory B	*10*
MYH10	Myosin heavy chain, nonmuscle IIB	*10*
MYLK	Myosin light chain kinase	*10*
P53	Tumor protein p53	*11*
PDE1C	Cyclic nucleotide phosphodiesterase 1 C	*1*
PDE2A	Phosphodiesterase 2A, cGMP-stimulated	*1*
PDE7A	High-affinity cAMP-specific 3′,5′-cyclic phosphodiesterase 7A	*1*
PRKAC	cAMP-dependent protein kinase catalytic subunit	*4*
PRKAR1B	cAMP-dependent protein kinase type I-beta regulatory subunit	*1*
RAP1	Ras-related protein Rap1	*1*
RYR1	Ryanodine receptor 1	*12*
STX7	Syntaxin-7	*1*
Tubulin	Tubulin	*1*

*1*References

Present study.

*2*Hoffert JD, Chou CL, Fenton RA, Knepper MA. Calmodulin is required for vasopressin-stimulated increase in cyclic AMP production in inner medullary collecting duct. J Biol Chem. 2005 Apr 8;280(14):13624–30.

*3*Helies-Toussaint C, Aarab L, Gasc JM, Verbavatz JM, Chabardes D. Cellular localization of type 5 and type 6 ACs in collecting duct and regulation of cAMP synthesis. Am J Physiol Renal Physiol. 2000 Jul;279(1):F185–94.

*4*Klussmann E, Maric K, Wiesner B, Beyermann M, Rosenthal W. Protein kinase A anchoring proteins are required for vasopressin-mediated translocation of aquaporin-2 into cell membranes of renal principal cells. J Biol Chem. 1999 Feb 19;274(8):4934–8.

*5*Fushimi K, Uchida S, Hara Y, Hirata Y, Marumo F, Sasaki S. Cloning and expression of apical membrane water channel of rat kidney collecting tubule. Nature. 1993 Feb 11;361(6412):549–52.

*6*Brooks HL, Ageloff S, Kwon TH, Brandt W, Terris JM, Seth A, Michea L, Nielsen S, Fenton R, Knepper MA. cDNA array identification of genes regulated in rat renal medulla in response to vasopressin infusion. Am J Physiol Renal Physiol. 2003 Jan;284(1):F218–28.

*7*Ostrowski NL, Young WS 3rd, Knepper MA, Lolait SJ. Expression of vasopressin V1a and V2 receptor messenger ribonucleic acid in the liver and kidney of embryonic, developing, and adult rats. Endocrinology. 1993 Oct;133(4):1849–59.

*8*Ecelbarger CA, Chou CL, Lee AJ, DiGiovanni SR, Verbalis JG, Knepper MA. Escape from vasopressin-induced antidiuresis: role of vasopressin resistance of the collecting duct. Am J Physiol. 1998 Jun;274(6 Pt 2):F1161–6.

*9*van Balkom BW, Hoffert JD, Chou CL, Knepper MA. Proteomic analysis of long-term vasopressin action in the inner medullary collecting duct of the Brattleboro rat. Am J Physiol Renal Physiol. 2004 Feb;286(2):F216–24.

*10*Chou CL, Christensen BM, Frische S, Vorum H, Desai RA, Hoffert JD, de Lanerolle P, Nielsen S, Knepper MA. Non-muscle myosin II and myosin light chain kinase are downstream targets for vasopressin signaling in the renal collecting duct. J Biol Chem. 2004 Nov 19;279(47):49026–35.

11 Hoorn EJ, Hoffert JD, Knepper MA. Combined proteomics and pathways analysis of collecting duct reveals a protein regulatory network activated in vasopressin escape. J Am Soc Nephrol. 2005 Oct;16(10):2852–63.

12 Chou CL, Yip KP, Michea L, Kador K, Ferraris JD, Wade JB, Knepper MA. Regulation of aquaporin-2 trafficking by vasopressin in the renal collecting duct. Roles of ryanodine-sensitive Ca2+ stores and calmodulin. J Biol Chem. 2000 Nov 24;275(47):36839–46.

Supplementary Table 5

Protein identifications in the flow-through fractions of biotin-avidin affinity purification from the dDAVP-infusion experiment in Brattleboro rats, included only proteins identified with 2 or more unique peptides (n = 630). A LTQ linear trap tandem mass spectrometer was used to analyze the samples.

Protein Name	Gene Name	Accession Number	Unique Peptide Number (Spectra Number)
Abl-interactor 1	ABI1	Q9QZM5	2 (4)
Acetylcholine receptor protein, delta subunit precursor	ACHD	P25110	2 (2)
Acetyl-CoA acetyltransferase, mitochondrial precursor	THIL	P17764	6 (37)
Acetyl-CoA carboxylase 1	COA1	P11497	3 (9)
Acidic leucine-rich nuclear phosphoprotein 32 family member A	AN32A	P49911	7 (10)
Aconitate hydratase, mitochondrial precursor	ACON	Q9ER34	24 (73)
Actin, alpha skeletal muscle	ACTS	P68136	20 (480)
Actin-related protein 2/3 complex subunit 1B	ARC1B	O88656	3 (7)
Activated RNA polymerase II transcriptional coactivator p15	TCP4	Q63396	3 (9)
Acyl coenzyme A thioester hydrolase, mitochondrial precursor	MTE1	O55171	2 (4)
Acyl-CoA dehydrogenase, medium-chain specific, mitochondrial precursor	ACADM	P08503	5 (8)
Acyl-CoA dehydrogenase, very-long-chain specific, mitochondrial precursor	ACADV	P45953	5 (18)
Acyl-CoA-binding protein	ACBP	P11030	2 (3)
Acyl-coenzyme A oxidase 2, peroxisomal	ACOX2	P97562	2 (2)
ADAM 7 precursor	AD07	Q63180	2 (16)
Adapter-related protein complex 1 beta 1 subunit	AP1B1	P52303	8 (27)
Adapter-related protein complex 2 alpha 2 subunit	AP2A2	P18484	8 (17)
Adapter-related protein complex 2 beta 1 subunit	A2B1	P62944	6 (20)
Adenine phosphoribosyltransferase	APT	P36972	5 (11)
Adenomatous polyposis coli protein	APC	P70478	7 (10)
Adenosine kinase	ADK	Q64640	2 (4)
Adenosylhomocysteinase	SAHH	P10760	8 (39)
Adenylate cyclase, type VIII	ADCY8	P40146	2 (2)
Adenylate kinase isoenzyme 1	KAD1	P39069	2 (3)
Adenylate kinase isoenzyme 2, mitochondrial	KAD2	P29410	3 (4)
Adenylyl cyclase-associated protein 1	CAP1	Q08163	9 (40)
ADP,ATP carrier protein 2	ADT2	Q09073	11 (63)
ADP-ribosylation factor 2	ARF2	P84082	5 (10)
ADP-ribosylation factor 4	ARF4	P61751	2 (5)
ADP-ribosylation factor 5	ARF5	P84083	4 (19)
ADP-ribosylation factor 6	ARF6	P62332	3 (6)
ADP-ribosylation factor-like protein 1	ARL1	P61212	2 (5)
Afadin	AFAD	O35889	3 (5)
Afadin- and alpha-actinin-binding protein	ADIP	Q8CGZ2	3 (9)
Aflatoxin B1 aldehyde reductase member 1	ARK71	P38918	6 (23)
A-kinase anchor protein 11	AK11	Q62924	2 (2)
A-kinase anchor protein 6	AKAP6	Q9WVC7	2 (2)
Alcohol dehydrogenase [NADP+]	AK1A1	P51635	4 (9)
Aldehyde dehydrogenase 1A3	AL1A3	Q8K4D8	16 (73)
Aldehyde dehydrogenase, cytosolic 1	ALDH1	P13601	3 (4)
Aldehyde dehydrogenase, dimeric NADP-preferring	AL3A1	P11883	2 (2)
Aldose reductase	ALDR	P07943	15 (171)
Alpha crystallin B chain	CRYAB	P23928	7 (21)
Alpha enolase	ENOA	P04764	17 (274)
Alpha-1-antiproteinase precursor	A1AT	P17475	2 (2)
Alpha-actinin 1	ACTN1	Q9Z1P2	18 (89)
Alpha-actinin 4	ACTN4	Q9QXQ0	18 (40)
Alpha-parvin	PARVA	Q9HB97	3 (5)
Amidophosphoribosyltransferase precursor	PUR1	P35433	2 (2)
Aminopeptidase B	AMPB	O09175	3 (7)
Anionic trypsin I precursor	TRY1	P00762	2 (36)
Annexin A1	ANXA1	P07150	25 (215)
Annexin A2	ANXA2	Q07936	24 (137)
Annexin A3	ANXA3	P14669	4 (12)
Annexin A4	ANXA4	P55260	12 (91)
Annexin A5	ANXA5	P14668	20 (156)
Annexin A6	ANXA6	P48037	20 (72)
Apoptosis regulator Bcl-X	BCLX	P53563	2 (2)
Aquaporin 1	AQP1	P29975	2 (8)
Aquaporin 2	AQP2	P34080	5 (25)
Arachidonate 15-lipoxygenase, type II	LX15B	Q8K4F2	3 (6)
ARF GTPase-activating protein GIT1	GIT1	Q9Z272	2 (5)
Arginase II, mitochondrial precursor	ARG2	O08701	8 (27)
Arylamine N-acetyltransferase 1	ARY1	P50297	2 (2)

Protein Name	Gene Name	Accession Number	Unique Peptide Number (Spectra Number)
Aspartate aminotransferase, cytoplasmic	AATC	P13221	5 (6)
Aspartate aminotransferase, mitochondrial precursor	AATM	P00507	8 (36)
ATP synthase alpha chain, mitochondrial precursor	ATPA	P15999	22 (156)
ATP synthase B chain, mitochondrial precursor	AT5F1	P19511	6 (8)
ATP synthase beta chain, mitochondrial precursor	ATPB	P10719	28 (164)
ATP synthase D chain, mitochondrial	ATP5H	P31399	7 (9)
ATP synthase gamma chain, mitochondrial	ATPG	P35435	2 (10)
ATP synthase oligomycin sensitivity conferral protein, mitochondrial precursor	ATPO	Q06647	10 (25)
ATP-binding cassette, sub-family A, member 2	ABC2	Q9ESR9	2 (2)
ATP-binding cassette, sub-family F, member 1	ABCF1	Q6MG08	2 (2)
ATP-citrate synthase	ACLY	P16638	2 (3)
ATP-dependent helicase DDX39	DDX39	Q5U216	4 (9)
Atrial natriuretic peptide receptor A precursor	ANPRA	P18910	2 (3)
Band 3 anion transport protein	B3AT	P23562	4 (17)
Barrier-to-autointegration factor	BAF	Q9R1T1	2 (3)
Bassoon protein	BSN	O88778	2 (7)
Beta-actin	ACTB	P60711	6 (186)
Beta-catenin	CTNB	Q9WU82	2 (12)
Bile salt export pump	AB11	O70127	3 (3)
Biliverdin reductase A precursor	BIEA	P46844	4 (10)
Breast cancer type 2 susceptibility protein homolog	BRCA2	O35923	5 (7)
Brevican core protein precursor	PGCB	P55068	2 (2)
C-1-tetrahydrofolate synthase, cytoplasmic	C1TC	P27653	4 (5)
Cadherin EGF LAG seven-pass G-type receptor 2	CELR2	Q9QYP2	2 (3)
Cadherin EGF LAG seven-pass G-type receptor 3	CELR3	O88278	2 (5)
Cadherin-23 precursor	CAD23	P58365	3 (5)
Calcineurin-binding protein Cabin 1	CABI	O88480	3 (9)
Calcium/calmodulin-dependent 3′,5′-cyclic nucleotide phosphodiesterase 1C	PDE1C	Q63421	2 (2)
Calcium/calmodulin-dependent protein kinase type II alpha chain	KCC2A	P11275	2 (3)
Calcium/calmodulin-dependent protein kinase type II delta chain	KCC2D	P15791	2 (3)
Calcium-binding protein p22	CHP1	P61023	2 (5)
Calgizzarin	S10AB	Q6B345	3 (43)
Calmodulin	CALM	P62161	4 (6)
Calnexin precursor	CALX	P35565	15 (47)
Calpactin I light chain	S110	P05943	2 (3)
Calpain small subunit 1	CPNS1	Q64537	5 (10)
Calpain-1 catalytic subunit	CAN1	P97571	15 (41)
Calpain-2 catalytic subunit	CAN2	Q07009	5 (8)
Calponin-3	CLP3	P37397	2 (11)
Calreticulin precursor	CRTC	P18418	6 (16)
cAMP-dependent protein kinase type I-beta regulatory subunit	KAP1	P81377	2 (3)
Cannabinoid receptor 2	CNR2	Q9QZN9	2 (4)
Carbonic anhydrase II	CAH2	P27139	6 (31)
Carbonyl reductase [NADPH] 1	DHCA	P47727	7 (14)
Carboxyl-terminal PDZ ligand of neuronal nitric oxide synthase protein	CPON	O54960	2 (2)
Carboxypeptidase D precursor	CBPD	Q9JHW1	2 (8)
Carnitine O-palmitoyltransferase I, mitochondrial liver isoform	CPT1A	P32198	4 (9)
Catalase	CATA	P04762	3 (6)
Catechol O-methyltransferase	COMT	P22734	4 (6)
Cathepsin B precursor	CATB	P00787	4 (6)
Cathepsin D precursor	CATD	P24268	7 (37)
CD166 antigen precursor	CD166	O35112	2 (3)
CD9 antigen	CD9	P40241	2 (7)
cGMP-dependent 3′,5′-cyclic phosphodiesterase	PDE2A	Q01062	2 (2)
cGMP-specific 3′,5′-cyclic phosphodiesterase	PDE5A	O54735	2 (5)
Clathrin coat assembly protein AP50	AP2M1	P84092	3 (3)
Clathrin heavy chain	CLH	P11442	43 (165)
Coatomer beta subunit	COPB	P23514	5 (5)
Coatomer beta′ subunit	COPB2	O35142	4 (19)
Cofilin-1	COF1	P45592	7 (43)
Complement C3 precursor [Contains: Complement C3 beta chain; Complement C3 alpha chain; C3a anaphylatoxin; Complement C3b alpha′ chain]	CO3	P01026	2 (6)
Complement component 1, Q subcomponent binding protein, mitochondrial precursor	MA32	O35796	2 (5)
Connector enhancer of kinase suppressor of ras 2	CNKR2	Q9Z1T4	2 (2)
Contactin associated protein 1 precursor	CTA1	P97846	2 (2)
Core histone macro-H2A.1	H2AY	Q02874	7 (16)
Coronin-1B	CO1B	O89046	2 (4)
Corticosteroid 11-beta-dehydrogenase, isozyme 2	DHI2	P50233	4 (13)

Protein Name	Gene Name	Accession Number	Unique Peptide Number (Spectra Number)
Creatine kinase, B chain	KCRB	P07335	8 (34)
Creatine kinase, ubiquitous mitochondrial precursor	KCRU	P25809	2 (3)
Cullin homolog 5	CUL5	Q9JJ31	2 (3)
Cyclin G1	CCNG1	P39950	3 (5)
Cysteine-rich protein 2	CRIP2	P36201	3 (8)
Cytochrome b5	CYB5	P00173	4 (6)
Cytochrome b5 outer mitochondrial membrane isoform precursor	CYM5	P04166	2 (2)
Cytochrome c oxidase polypeptide Va, mitochondrial precursor	COX5A	P11240	2 (3)
Cytochrome c oxidase subunit 2	COX2	P00406	2 (6)
Cytochrome c oxidase subunit IV isoform 1, mitochondrial precursor	COX41	P10888	3 (6)
Cytochrome c, somatic	CYC	P62898	3 (9)
Cytochrome P450 1A1	CP1A1	P00185	2 (10)
Cytochrome P450 24A1, mitochondrial precursor	CP24A	Q09128	2 (2)
Cytochrome P450 2C22	CP2CM	P19225	2 (2)
Cytochrome P450 4B1	CP4B1	P15129	2 (8)
D-3-phosphoglycerate dehydrogenase	SERA	O08651	2 (2)
D-dopachrome tautomerase	DOPD	P80254	4 (7)
Death effector domain-containing protein	DEDD	Q9Z2K0	2 (2)
Defender against cell death 1	DAD1	P61805	2 (6)
Deubiquitinating protein VCIP135	VCIP1	Q8CF97	2 (2)
Dihydrolipoyllysine-residue acetyltransferase component of pyruvate dehydrogenase complex	ODP2	P08461	3 (10)
Dihydrolipoyllysine-residue succinyltransferase component of 2-oxoglutarate dehydrogenase complex, mitochondrial precursor	ODO2	Q01205	2 (3)
Dihydropyrimidinase related protein-2	DPYL2	P47942	4 (9)
Dihydroxyacetone phosphate acyltransferase	GNPAT	Q9ES71	3 (3)
Dipeptidyl-peptidase III	DPP3	O55096	2 (3)
Disks large-associated protein 4	DLP4	P97839	2 (6)
DJ-1 protein	PARK7	O88767	4 (11)
DNA (cytosine-5)-methyltransferase 1	DNMT1	Q9Z330	2 (2)
DNA polymerase gamma subunit 1	DPOG1	Q9QYV8	2 (3)
Dolichyl-diphosphooligosaccharide--protein glycosyltransferase 63 kDa subunit precursor	RIB2	P25235	6 (22)
Dolichyl-diphosphooligosaccharide--protein glycosyltransferase 67 kDa subunit precursor	RIB1	P07153	5 (8)
Drebrin-like protein	DBNL	Q9JHL4	3 (10)
Dynein heavy chain, cytosolic	DYHC	P38650	34 (75)
Dynein intermediate chain 2, cytosolic	DYI2	Q62871	2 (10)
E3 ubiquitin-protein ligase Nedd-4	NEDD4	Q62940	4 (8)
Electron transfer flavoprotein alpha-subunit, mitochondrial precursor	ETFA	P13803	7 (24)
Elongation factor 1-alpha 1	EF1A1	P62630	4 (20)
Elongation factor 1-alpha 2	EF1A2	P62632	6 (67)
Elongation factor 1-gamma	EF1G	Q68FR6	5 (11)
Elongation factor 2	EF2	P05197	15 (71)
Endoplasmic reticulum protein ERp29 precursor	ERP29	P52555	3 (5)
Enoyl-CoA hydratase, mitochondrial precursor	ECHM	P14604	2 (4)
Epithelial-cadherin precursor	CADH1	Q9R0T4	4 (14)
ERC protein 2	ERC2	Q8K3M6	2 (3)
Eukaryotic translation initiation factor 2 subunit 1	IF2A	P68101	2 (3)
Eukaryotic translation initiation factor 2C 2	I2C2	Q9QZ81	2 (3)
Eukaryotic translation initiation factor 4E	IF4E	P63074	2 (2)
Ezrin	EZRI	P31977	2 (7)
Fanconi anemia group C protein homolog	FANCC	O35870	2 (3)
Far upstream element binding protein 2	FUBP2	Q99PF5	3 (9)
Fatty acid synthase [Includes: [Acyl-carrier-protein] S-acetyltransferase	FAS	P12785	7 (11)
Fatty acid-binding protein, heart	FABH	P07483	4 (6)
Fatty aldehyde dehydrogenase	AL3A2	P30839	3 (5)
Ferritin heavy chain	FRIH	P19132	4 (8)
Flotillin-1	FLOT1	Q9Z1E1	4 (12)
Focal adhesion kinase 1	FAK1	O35346	4 (4)
Follitropin beta chain precursor	FSHB	P18427	2 (3)
Fructose-bisphosphate aldolase A	ALDOA	P05065	9 (54)
Fumarate hydratase, mitochondrial precursor	FUMH	P14408	3 (5)
Galectin-1	LEG1	P11762	2 (3)
Galectin-3	LEG3	P08699	3 (8)
Gamma-glutamyltranspeptidase 1 precursor	GGT1	P07314	2 (6)
General vesicular transport factor p115	VDP	P41542	4 (7)
Glia maturation factor beta	GLMB	Q63228	3 (4)
Glial fibrillary acidic protein, astrocyte	GFAP	P47819	2 (17)
Glucose-6-phosphate 1-dehydrogenase	G6PD	P05370	2 (3)
Glutamate [NMDA] receptor subunit epsilon 1 precursor	NMDE1	Q00959	2 (2)
Glutamate dehydrogenase 1, mitochondrial precursor	DHE3	P10860	8 (23)

Protein Name	Gene Name	Accession Number	Unique Peptide Number (Spectra Number)
Glutamate receptor 1 precursor	GRIA1	P19490	2 (3)
Glutamate receptor, ionotropic kainate 4 precursor	GRIK4	Q01812	2 (2)
Glutaminase, kidney isoform, mitochondrial precursor	GLSK	P13264	2 (4)
Glutathione peroxidase	GPX1	P04041	9 (22)
Glutathione peroxidase-gastrointestinal	GPX2	P83645	5 (9)
Glutathione S-transferase Mu 1	GSTM1	P04905	14 (145)
Glutathione S-transferase Mu 2	GSTM2	P08010	20 (134)
Glutathione S-transferase P	GSTP1	P04906	6 (78)
Glutathione S-transferase theta 2	GSTT2	P30713	2 (4)
Glutathione S-transferase Yb-3	GSTM4	P08009	2 (2)
Glutathione synthetase	GSHB	P46413	2 (4)
Glyceraldehyde-3-phosphate dehydrogenase	G3P	P04797	11 (146)
Glycerol-3-phosphate dehydrogenase, mitochondrial precursor	GPDM	P35571	2 (6)
Glycogen phosphorylase, brain form	PHS3	P53534	17 (65)
Glycogen phosphorylase, liver form	PHS1	P09811	6 (13)
Glycogen phosphorylase, muscle form	PHS2	P09812	4 (4)
Golgi apparatus protein 1 precursor	GLG1	Q62638	2 (2)
Golgi autoantigen, golgin subfamily A member 2	GOA2	Q62839	3 (4)
Golgi reassembly stacking protein 2	GORS2	Q9R064	2 (3)
GPI transamidase component PIG-S	PIGS	Q5XI31	3 (4)
GrpE protein homolog 1, mitochondrial precursor	GRE1	P97576	2 (3)
GTP:AMP phosphotransferase mitochondrial	KAD3	P29411	4 (7)
GTPase activating RapGAP domain-like 1	GRIP	O55007	2 (5)
GTP-binding nuclear protein Ran	RAN	P62828	5 (11)
Guanine nucleotide-binding protein beta subunit 2-like 1	GBLP	P63245	4 (8)
Guanine nucleotide-binding protein G(i), alpha-1 subunit	GNAI1	P10824	2 (2)
Guanine nucleotide-binding protein G(i), alpha-2 subunit	GNAI2	P04897	2 (3)
Guanine nucleotide-binding protein G(I)/G(S)/G(O) gamma-8 subunit	GBG8	P63077	3 (3)
Guanine nucleotide-binding protein G(s), alpha subunit	GNAS	P63095	2 (4)
Guanine nucleotide-binding protein, alpha-11 subunit	GB11	Q9JID2	3 (5)
Hamartin	TSC1	Q9Z136	2 (3)
Heat shock 70 kDa protein 1A/1B	HSP71	Q07439	23 (120)
Heat shock 70 kDa protein 1L	HS7L	P55063	2 (2)
Heat shock cognate 71 kDa protein	HSP7C	P63018	25 (156)
Heat shock protein HSP 90-beta	HS9B	P34058	33 (156)
Heat shock-related 70 kDa protein 2	HSP72	P14659	8 (36)
Heat-shock protein beta-1	HSB1	P42930	6 (30)
Heterogeneous nuclear ribonucleoprotein A1	ROA1	P04256	2 (12)
Heterogeneous nuclear ribonucleoprotein A3	ROA3	Q6URK4	5 (40)
Heterogeneous nuclear ribonucleoprotein D0	HNRPD	Q9JJ54	4 (12)
Heterogeneous nuclear ribonucleoprotein K	HNRPK	P61980	13 (46)
Heterogeneous nuclear ribonucleoprotein Q	HNRPQ	Q7TP47	3 (4)
Hexokinase, type I	HXK1	P05708	16 (42)
High mobility group protein 1	HMG1	P63159	7 (16)
High-affinity cAMP-specific 3′,5′-cyclic phosphodiesterase 7A	CN7A	O08593	2 (2)
Hippocalcin-like protein 1	HPCL1	P62749	3 (7)
Histone H1.0	H10	P43278	3 (15)
Histone H1.2	H12	P15865	5 (44)
Histone H1t	H1T	P06349	3 (11)
Histone H2A.1	H2A1	P02262	5 (151)
Histone H2A.z	H2AZ	P17317	2 (6)
Histone H2B	H2B	Q00715	7 (98)
Histone H2B, testis	H2BT	Q00729	3 (69)
Histone H3.3	H33	P84245	4 (17)
Histone H4	H4	P62804	12 (319)
Hsc70-interacting protein	ST13	P50503	3 (3)
Huntingtin	HD	P51111	3 (8)
Huntingtin associated protein 1	HAP1	P54256	3 (9)
Hypoxanthine-guanine phosphoribosyltransferase	HPRT	P27605	4 (9)
Importin beta-1 subunit	IMB1	P52296	4 (8)
Inhibitor of nuclear factor kappa B kinase beta subunit	IKKB	Q9QY78	3 (3)
Inositol 1,4,5-trisphosphate receptor type 1	ITPR1	P29994	4 (4)
Inositol 1,4,5-trisphosphate receptor type 2	ITPR2	P29995	2 (3)
Inositol 1,4,5-trisphosphate receptor type 3	ITPR3	Q63269	2 (2)
Inositol monophosphatase	IMPA1	P97697	2 (5)
Integrin alpha-7	ITA7	Q63258	3 (5)
Integrin beta-1 precursor	ITB1	P49134	5 (12)
Inter-alpha-trypsin inhibitor heavy chain H3 precursor	ITIH3	Q63416	2 (3)
Interferon-induced guanylate-binding protein 2	GBP2	Q63663	2 (4)
Iron-responsive element binding protein 1	IREB1	Q63270	4 (10)
Isocitrate dehydrogenase [NADP] cytoplasmic	IDHC	P41562	11 (30)
Kelch-like protein 10	KLH10	Q6JEL3	3 (3)

Protein Name	Gene Name	Accession Number	Unique Peptide Number (Spectra Number)
Keratin, type I cytoskeletal 19	K1C19	Q63279	17 (46)
Keratin, type I cytoskeletal 21	K1C21	P25030	2 (7)
Keratin, type II cytoskeletal 1b	K2C1B	Q6IG01	4 (10)
Keratin, type II cytoskeletal 8	K2C8	Q10758	22 (145)
Kinesin light chain 1	KLC1	P37285	3 (3)
Lamin A	LAMA	P48679	10 (18)
Lamin B1	LAM1	P70615	7 (15)
Laminin beta-2 chain precursor	LMB2	P15800	14 (45)
Leucine zipper-EF-hand containing transmembrane protein 1, mitochondrial precursor	LETM1	Q5XIN6	2 (2)
Leukotriene A-4 hydrolase	LKHA4	P30349	7 (9)
LIM and SH3 domain protein 1	LAS1	Q99MZ8	2 (2)
L-lactate dehydrogenase A chain	LDHA	P04642	23 (254)
L-lactate dehydrogenase B chain	LDHB	P42123	3 (8)
Long-chain-fatty-acid--CoA ligase 4	ACSL4	O35547	2 (2)
Long-chain-fatty-acid--CoA ligase 5	ACSL5	O88813	2 (5)
Loss of heterozygosity 11 chromosomal region 2 gene A protein homolog	LHR2A	Q75WE7	4 (7)
Low molecular weight phosphotyrosine protein phosphatase	PPAC	P41498	2 (5)
Lupus La protein homolog	LA	P38656	4 (6)
Lutropin-choriogonadotropic hormone receptor precursor	LSHR	P16235	2 (2)
L-xylulose reductase	DCXR	Q920P0	3 (10)
Lysosomal acid phosphatase precursor	PPAL	P20611	2 (4)
Macrophage migration inhibitory factor	MIF	P30904	2 (66)
Major vault protein	MVP	Q62667	15 (38)
Malate dehydrogenase, mitochondrial precursor	MDHM	P04636	10 (70)
Mast cell protease IV precursor	MCPT4	P97592	2 (14)
Matrin 3	MATR3	P43244	3 (5)
Melanoma-associated antigen D1	MAGD1	Q9ES73	2 (5)
Membrane associated progesterone receptor component 1	PGRC1	P70580	3 (4)
Merlin	MERL	Q63648	3 (4)
Metabotropic glutamate receptor 4 precursor	MGR4	P31423	2 (2)
Methylmalonate-semialdehyde dehydrogenase [acylating], mitochondrial precursor	MMSA	Q02253	8 (32)
Microsomal signal peptidase 18 kDa subunit	SPC4	P42667	2 (3)
Mitochondrial 2-oxoglutarate/malate carrier protein	M2OM	P97700	4 (5)
Moesin	MOES	O35763	5 (40)
Monoglyceride lipase	MGLL	Q8R431	2 (2)
Multidrug resistance protein 1	MDR1	P43245	3 (4)
Myogenin	MYOG	P20428	2 (5)
Myosin heavy chain, cardiac muscle beta isoform	MYH7	P02564	5 (8)
Myosin heavy chain, fast skeletal muscle, embryonic	MYH3	P12847	4 (8)
Myosin heavy chain, nonmuscle IIA	MYH9	Q62812	51 (221)
Myosin heavy chain, nonmuscle IIB	MYH10	Q9JLT0	60 (230)
Myosin Ib	MYO1B	Q05096	2 (3)
Myosin Id	MYO1D	Q63357	4 (6)
Myosin light polypeptide 6	MYL6	Q64119	10 (33)
Myosin regulatory light chain 2, smooth muscle isoform	MLRN	Q64122	5 (9)
Myosin regulatory light chain 2-A, smooth muscle isoform	MLRA	P13832	2 (4)
Myosin regulatory light chain 2-B, smooth muscle isoform	MLRB	P18666	4 (13)
Myosin Va	MYO5A	Q9QYF3	3 (5)
Myotrophin	MTPN	P62775	2 (2)
NACHT-, LRR- and PYD-containing protein 6	NALP6	Q63035	2 (5)
NADH-cytochrome b5 reductase	NCB5R	P20070	3 (6)
NADH-ubiquinone oxidoreductase 24 kDa subunit, mitochondrial precursor	NUHM	P19234	3 (6)
NADP-dependent leukotriene B4 12-hydroxydehydrogenase	LTB4D	P97584	6 (39)
NADP-dependent malic enzyme	MAOX	P13697	2 (6)
Neurabin-I	NEB1	O35867	2 (3)
Neurogenic locus notch homolog protein 1 precursor	NOTC1	Q07008	2 (5)
Neurogenic locus notch homolog protein 2 precursor	NOTC2	Q9QW30	2 (3)
Neurogenic locus notch homolog protein 3 precursor	NOTC3	Q9R172	2 (2)
NSFL1 cofactor p47	NSF1C	O35987	2 (5)
Nuclease sensitive element binding protein 1	YBOX1	P62961	2 (17)
Nucleolar phosphoprotein p130	NOLC1	P41777	2 (2)
Nucleolar protein NOP5	NOP5	Q9QZ86	2 (4)
Nucleolin	NUCL	P13383	6 (15)
Nucleophosmin	NPM	P13084	2 (2)
Nucleoside diphosphate kinase A	NDKA	Q05982	3 (9)
Nucleoside diphosphate kinase B	NDKB	P19804	5 (12)
Nucleosome assembly protein 1-like 1	NPL1	Q9Z2G8	3 (5)
Olfactory guanylyl cyclase GC-D precursor	GUC2D	P51839	2 (3)
Ornithine aminotransferase, mitochondrial precursor	OAT	P04182	4 (8)

Protein Name	Gene Name	Accession Number	Unique Peptide Number (Spectra Number)
Ornithine decarboxylase	DCOR	P09057	2 (3)
Parathymosin	PTMS	P04550	2 (4)
Partitioning-defective 3 homolog	PARD3	Q9Z340	2 (12)
PDZ domain containing protein 3	PDZK3	Q9QZR8	2 (3)
PDZ domain containing RING finger protein 3	PZRN3	P68907	3 (7)
Peptidyl-prolyl cis-trans isomerase A	PPIA	P10111	6 (61)
Peptidyl-prolyl cis-trans isomerase B precursor	PPIB	P24368	7 (17)
Peripherin	RDS	P17438	3 (4)
Peroxiredoxin 1	PRDX1	Q63716	9 (43)
Peroxiredoxin 2	PRDX2	P35704	9 (44)
Peroxiredoxin 5, mitochondrial precursor	PRDX5	Q9R063	13 (54)
Peroxiredoxin 6	PRDX6	O35244	13 (39)
Peroxisomal multifunctional enzyme type 2	DHB4	P97852	4 (4)
Phosphate carrier protein, mitochondrial precursor	MPCP	P16036	4 (23)
Phosphatidylethanolamine-binding protein	PEBP	P31044	8 (49)
Phosphatidylinositol 3-kinase regulatory alpha subunit	P85A	Q63787	2 (3)
Phosphatidylinositol-4,5-bisphosphate 3-kinase catalytic subunit, beta isoform	P11B	Q9Z1L0	2 (9)
Phosphatidylinositol-binding clathrin assembly protein	PICA	O55012	3 (17)
Phosphoglucomutase	PGMU	P38652	4 (11)
Phosphoglycerate kinase 1	PGK1	P16617	11 (74)
Phosphoglycerate mutase 1	PMG1	P25113	4 (23)
Piccolo protein	PCLO	Q9JKS6	2 (3)
Plasma membrane calcium-transporting ATPase 1	AT2B1	P11505	3 (6)
Plasma membrane calcium-transporting ATPase 2	AT2B2	P11506	2 (2)
Plasma membrane calcium-transporting ATPase 4	AT2B4	Q64542	2 (2)
Platelet-activating factor acetylhydrolase IB alpha subunit	LIS1	P63004	2 (3)
Platelet-activating factor acetylhydrolase IB beta subunit	PA1B2	O35264	3 (7)
Plectin 1	PLEC1	P30427	78 (209)
Poly [ADP-ribose] polymerase-1	PARP1	P27008	2 (2)
Polyadenylate-binding protein 1	PABP1	Q9EPH8	3 (5)
Polypyrimidine tract-binding protein 1	PTBP1	Q00438	3 (11)
Potassium voltage-gated channel subfamily H member 5	KCNH5	Q9EPI9	2 (2)
Potassium voltage-gated channel subfamily H member 6	KCNH6	O54853	2 (2)
Potassium voltage-gated channel subfamily KQT member 3	CIQ3	O88944	2 (2)
Potassium-transporting ATPase alpha chain 2	AT12A	P54708	2 (2)
POU domain, class 3, transcription factor 1	PO3F1	P20267	2 (5)
PRA1 family protein 3	PRA3	Q9ES40	3 (6)
PR-domain zinc finger protein 2	PRDM2	Q63755	2 (3)
Probable alcohol sulfotransferase	SUH2	P07631	2 (2)
Pro-epidermal growth factor precursor	EGF	P07522	2 (15)
Profilin-1	PROF1	P62963	10 (44)
Programmed cell death 6 interacting protein	PD6I	Q9QZA2	5 (11)
Programmed cell death protein 8, mitochondrial precursor	PDCD8	Q9JM53	6 (10)
Prohibitin	PHB	P67779	6 (8)
Propionyl-CoA carboxylase alpha chain, mitochondrial precursor	PCCA	P14882	5 (5)
Propionyl-CoA carboxylase beta chain, mitochondrial precursor	PCCB	P07633	12 (49)
Prostaglandin F2-alpha receptor	PF2R	P43118	2 (4)
Prostaglandin G/H synthase 1 precursor	PGH1	Q63921	8 (34)
Prostaglandin G/H synthase 2 precursor	PGH2	P35355	2 (2)
Proteasome activator complex subunit 1	PSE1	Q63797	12 (38)
Proteasome activator complex subunit 2	PSME2	Q63798	4 (15)
Proteasome subunit alpha type 1	PSA1	P18420	3 (3)
Proteasome subunit alpha type 2	PSA2	P17220	2 (6)
Proteasome subunit alpha type 3	PSA3	P18422	4 (7)
Proteasome subunit alpha type 5	PSA5	P34064	4 (9)
Proteasome subunit alpha type 6	PSA6	P60901	5 (11)
Proteasome subunit beta type 1	PSB1	P18421	5 (9)
Proteasome subunit beta type 3	PSB3	P40112	2 (4)
Proteasome subunit beta type 4 precursor	PSB4	P34067	2 (5)
Proteasome subunit beta type 5 precursor	PSB5	P28075	2 (4)
Proteasome subunit beta type 8 precursor	PSB8	P28064	2 (2)
Protein disulfide-isomerase A3 precursor	PDIA3	P11598	24 (87)
Protein disulfide-isomerase A4 precursor	PDIA4	P38659	3 (3)
Protein disulfide-isomerase A6 precursor	PDIA6	Q63081	4 (25)
Protein disulfide-isomerase precursor	PDIA1	P04785	13 (21)
Protein kinase C and casein kinase substrate in neurons 2 protein	PACN2	Q9QY17	3 (5)
Protein kinase C, epsilon type	KPCE	P09216	2 (6)
Protein phosphatase 1 regulatory subunit 10	PP1RA	O55000	2 (10)
Protein phosphatase 1 regulatory subunit 12A	MPT1	Q10728	2 (2)
Protein-glutamine gamma-glutamyltransferase K	TGM1	P23606	4 (4)
Protein-L-isoaspartate(D-aspartate) O-methyltransferase	PIMT	P22062	2 (2)

Protein Name	Gene Name	Accession Number	Unique Peptide Number (Spectra Number)
Protocadherin Fat 2 precursor	FAT2	O88277	3 (4)
Proto-oncogene C-crk	CRK	Q63768	3 (11)
PRP19/PSO4 homolog	PRP19	Q9JMJ4	2 (3)
Pyrroline-5-carboxylate reductase 2	P5CR2	Q6AY23	3 (9)
Pyruvate dehydrogenase E1 component alpha subunit, somatic form, mitochondrial precursor	ODPA	P26284	2 (17)
Pyruvate dehydrogenase E1 component beta subunit, mitochondrial precursor	ODPB	P49432	3 (13)
Pyruvate kinase, isozymes M1/M2	KPYM	P11980	32 (350)
Rab GDP dissociation inhibitor alpha	GDIA	P50398	8 (23)
Rab GDP dissociation inhibitor beta-2	GDIC	P50399	8 (31)
Rab GTPase binding effector protein 2	RABEP2	Q62835	3 (5)
RAB6 interacting protein 2	RB6I2	Q811U3	4 (4)
Rap guanine nucleotide exchange factor 3	RPGF3	Q9Z1C8	3 (3)
Ras GTPase-activating protein 2	RSG2	Q63713	3 (3)
Ras-related C3 botulinum toxin substrate 1	RAC1	Q6RUV5	4 (9)
Ras-related protein Rab-11A	RB11A	P62494	7 (18)
Ras-related protein Rab-11B	RB11B	O35509	3 (7)
Ras-related protein Rab-14	RAB14	P61107	2 (5)
Ras-related protein Rab-1A	RAB1A	Q6NYB7	4 (12)
Ras-related protein Rab-1B	RAB1B	P10536	3 (6)
Ras-related protein Rab-2A	RB2A	P05712	5 (16)
Ras-related protein Rab-7	RAB7	P09527	7 (26)
Ras-related protein Rab-8A	RAB8A	P35280	2 (2)
Ras-related protein Ral-A	RALA	P63322	2 (3)
Ras-related protein Rap-1b	RAP1B	Q62636	4 (20)
Regulator of G-protein signaling 12	RGS12	O08774	4 (5)
Reticulon 4	RTN4	Q9JK11	7 (33)
Retinal dehydrogenase 1	AL1A1	P51647	15 (128)
Retinoblastoma-like protein 2	RBL2	O55081	2 (4)
Retinoic acid receptor RXR-beta	RXRB	P49743	2 (2)
Retinoid-inducible serine carboxypeptidase precursor	RISC	Q920A6	3 (6)
Rho guanine nucleotide exchange factor 1	ARHG1	Q9Z1I6	3 (3)
Rho guanine nucleotide exchange factor 11	ARHGB	Q9ES67	2 (3)
Rho-associated protein kinase 1	ROCK1	Q63644	2 (3)
Rho-interacting protein 3	RIP3	Q9ERE6	2 (6)
Rho-related GTP-binding protein RhoB	RHOB	P62747	2 (3)
Ribonuclease inhibitor	RINI	P29315	4 (13)
Ribonuclease UK114	UK14	P52759	3 (5)
Ribosomal protein S6 kinase alpha 1	KS6A1	Q63531	3 (14)
RT1 class I histocompatibility antigen, AA alpha chain precursor	HA12	P16391	2 (5)
S100 calcium-binding protein A4	S10A4	P05942	3 (38)
S-100 protein, alpha chain	S10A1	P35467	3 (43)
Sarcoplasmic/endoplasmic reticulum calcium ATPase 1	AT2A1	Q64578	2 (5)
Sarcoplasmic/endoplasmic reticulum calcium ATPase 2	AT2A2	P11507	6 (12)
Scavenger mRNA decapping enzyme DcpS	DCPS	Q8K4F7	3 (6)
Semaphorin 6C precursor	SEM6C	Q9WTL3	3 (4)
Senescence marker protein-30	SM30	Q03336	2 (2)
Sepiapterin reductase	SPRE	P18297	2 (5)
Septin 7	SEPT7	Q9WVC0	3 (7)
Septin 9	SEPT9	Q9QZR6	2 (4)
Serine/threonine protein phosphatase 5	PPP5	P53042	2 (6)
Serine/threonine protein phosphatase PP1-gamma catalytic subunit	PP1G	P63088	2 (9)
Serine/threonine-protein kinase MARK1	MARK1	O08678	2 (2)
Serine/threonine-protein kinase PAK 1	PAK1	P35465	2 (2)
Serine/threonine-protein kinase PLK1	PLK1	Q62673	2 (2)
Serine/threonine-protein kinase WNK4	WNK4	Q7TPK6	3 (4)
Serotransferrin precursor	TRFE	P12346	4 (4)
Serum albumin precursor	ALBU	P02770	6 (39)
SET protein	SET	Q63945	3 (7)
SH3 and multiple ankyrin repeat domains protein 2	SHAN2	Q9QX74	2 (2)
Short chain 3-hydroxyacyl-CoA dehydrogenase, mitochondrial precursor	HCDH	Q9WVK7	2 (6)
Sideroflexin 3	SFX3	Q9JHY2	2 (2)
Signal transducer and activator of transcription 3	STAT3	P52631	6 (9)
Sodium channel protein type IX alpha subunit	SCN9A	O08562	2 (3)
Sodium channel protein type XI alpha subunit	SC11A	O88457	2 (4)
Sodium/glucose cotransporter 1	SC5A1	P53790	2 (3)
Sodium/potassium-transporting ATPase alpha-1 chain precursor	AT1A1	P06685	26 (188)
Sodium/potassium-transporting ATPase alpha-2 chain precursor	AT1A2	P06686	2 (3)
Sodium/potassium-transporting ATPase alpha-3 chain	AT1A3	P06687	9 (94)
Sodium/potassium-transporting ATPase alpha-4 chain	AT1A4	Q64541	5 (19)
Sodium/potassium-transporting ATPase beta-1 chain	AT1B1	P07340	7 (37)

Protein Name	Gene Name	Accession Number	Unique Peptide Number (Spectra Number)
Sodium-dependent dopamine transporter	S6A3	P23977	2 (4)
Solute carrier family 12, member 5	S12A5	Q63633	2 (2)
Solute carrier family 2, facilitated glucose transporter, member 1	GTR1	P11167	2 (8)
Sorting nexin 1	SNX1	Q99N27	3 (3)
Spectrin alpha chain, brain	SPTA2	P16086	93 (324)
Spectrin beta chain, brain 2	SPTN2	Q9QWN8	46 (181)
S-phase kinase-associated protein 1A	SKP1	Q6PEC4	4 (8)
Sphingosine-1-phosphate lyase 1	SGP1	Q8CHN6	2 (4)
Squalene monooxygenase	ERG1	P52020	3 (5)
Staphylococcal nuclease domain containing protein 1	SND1	Q66X93	3 (4)
Stathmin 2	STMN2	P21818	2 (2)
Stress-70 protein, mitochondrial precursor	GRP75	P48721	8 (20)
Stress-induced-phosphoprotein 1	STIP1	O35814	4 (11)
Structural maintenance of chromosome 1-like 1 protein	SMC1A	Q9Z1M9	4 (5)
Structural maintenance of chromosome 3	SMC3	P97690	2 (2)
Succinate dehydrogenase [ubiquinone] flavoprotein subunit, mitochondrial precursor	DHSA	Q920L2	6 (10)
Sulfated glycoprotein 1 precursor	SAP	P10960	5 (9)
Sulfonylurea receptor 2	ACC9	Q63563	4 (5)
Superoxide dismutase [Cu-Zn]	SODC	P07632	4 (17)
Superoxide dismutase [Mn], mitochondrial precursor	SODM	P07895	3 (8)
Synaptic glycoprotein SC2	GPSN2	Q64232	4 (11)
Synaptonemal complex protein 1	SYCP1	Q03410	3 (3)
Synaptonemal complex protein 2	SYCP2	O70608	3 (4)
Synaptotagmin-like protein 5	SYTL5	Q812E4	2 (5)
T-complex protein 1, alpha subunit	TCPA	P28480	5 (13)
T-complex protein 1, delta subunit	TCPD	Q7TPB1	5 (29)
TGF-beta receptor type I precursor	TGFR1	P80204	2 (2)
Thimet oligopeptidase	MEPD	P24155	2 (3)
Thioredoxin	THIO	P11232	3 (5)
Thioredoxin reductase 1, cytoplasmic	TRXR1	O89049	3 (10)
Threonyl-tRNA synthetase, cytoplasmic	SYTC	Q5XHY5	3 (4)
Thyroglobulin precursor	THYG	P06882	3 (29)
T-plastin	PLST	Q63598	20 (75)
Transaldolase	TAL1	Q9EQS0	8 (16)
Transferrin receptor protein 1	TFR1	Q99376	2 (3)
Trans-Golgi network integral membrane protein TGN38 precursor	TGON3	P19814	2 (3)
Transient receptor potential cation channel subfamily M member 8	TCM8	Q8R455	2 (2)
Transitional endoplasmic reticulum ATPase	TERA	P46462	13 (37)
Transketolase	TKT	P50137	9 (37)
Translation initiation factor eIF-2B gamma subunit	EI2BG	P70541	2 (3)
Translationally controlled tumor protein	TCTP	P63029	3 (4)
Transmembrane 9 superfamily protein member 2 precursor	TM9S2	Q66HG5	5 (19)
Transmembrane protein Tmp21 precursor	TMP21	Q63584	3 (4)
Trifunctional enzyme alpha subunit, mitochondrial precursor	ECHA	Q64428	14 (50)
Trifunctional enzyme beta subunit, mitochondrial precursor	ECHB	Q60587	5 (15)
Triosephosphate isomerase	TPIS	P48500	14 (65)
Tropomyosin 1 alpha chain	TPM1	P04692	10 (44)
Tropomyosin alpha 4 chain	TPM4	P09495	5 (23)
Tropomyosin beta chain	TPM2	P58775	4 (15)
Tuberin	TSC2	P49816	4 (4)
Tubulin alpha-1 chain	TBA1	P68370	14 (206)
Tubulin alpha-2 chain	TBA2	Q6P9V9	2 (11)
TUBULIN BETA CHAIN	TBB1	P04691	3 (31)
Tubulin beta-5 chain	TBB5	P69897	20 (152)
Tumor protein D54	TPD54	Q6PCT3	3 (6)
Ubiquinol-cytochrome c reductase iron-sulfur subunit, mitochondrial precursor	UCRI	P20788	2 (2)
Ubiquinol-cytochrome-c reductase complex core protein 2, mitochondrial precursor	UQCR2	P32551	7 (18)
Ubiquitin	UBIQ	P62989	5 (28)
Ubiquitin-conjugating enzyme E2 variant 2	UB2V2	Q7M767	3 (8)
UDP-glucose 6-dehydrogenase	UGDH	O70199	2 (3)
Urotensin-2B precursor	UTS2B	Q765I2	4 (4)
Vacuolar ATP synthase subunit B, brain isoform	VATB2	P62815	2 (4)
Vesicle-associated membrane protein-associated protein A	VAPA	Q9Z270	3 (4)
Vigilin	VIGLN	Q9Z1A6	3 (4)
Vimentin	VIME	P31000	9 (21)
Voltage-dependent anion-selective channel protein 1	VDAC1	Q9Z2L0	9 (25)
Voltage-dependent anion-selective channel protein 2	VDAC2	P81155	6 (14)
Voltage-dependent anion-selective channel protein 3	VDAC3	Q9R1Z0	3 (8)
Voltage-dependent L-type calcium channel alpha-1C subunit	CAC1C	P22002	2 (4)

Protein Name	Gene Name	Accession Number	Unique Peptide Number (Spectra Number)
Voltage-dependent T-type calcium channel alpha-1G subunit	CAC1G	O54898	2 (2)
WD-repeat protein 56	WDR56	Q66HB3	2 (2)
Zinc phosphodiesterase ELAC protein 2	RNZ2	Q8CGS5	2 (8)
[Segment 1 of 2] Myosin heavy chain, smooth muscle isoform	Myh11	Q63862_1	6 (24)
[Segment 1 of 2] Versican core protein precursor	Cspg2	Q9ERB4_1	2 (3)
[Segment 2 of 2] Myosin heavy chain, smooth muscle isoform	Myh11	Q63862_2	5 (22)
10 kDa heat shock protein, mitochondrial	CH10	P26772	3 (4)
10-formyltetrahydrofolate dehydrogenase	FTHFD	P28037	2 (3)
14-3-3 protein beta/alpha	1433B	P35213	3 (7)
14-3-3 protein epsilon	1433E	P62260	4 (66)
14-3-3 protein eta	1433F	P68511	4 (9)
14-3-3 protein gamma	143G	P61983	2 (6)
14-3-3 protein tau	1433T	P68255	11 (98)
14-3-3 protein zeta/delta	143Z	P63102	8 (137)
15 kDa selenoprotein precursor	SEP15	Q923V8	2 (2)
150 kDa oxygen-regulated protein precursor	OXRP	Q63617	3 (3)
1-phosphatidylinositol-4,5-bisphosphate phosphodiesterase beta 3	PIB3	Q99JE6	2 (2)
1-phosphatidylinositol-4,5-bisphosphate phosphodiesterase gamma 2	PLCG2	P24135	2 (2)
2,4-dienoyl-CoA reductase, mitochondrial precursor	DECR	Q64591	5 (12)
26S protease regulatory subunit 6A	PRS6A	Q63569	3 (18)
26S protease regulatory subunit 6B	PRS6B	Q63570	4 (9)
26S protease regulatory subunit 8	PRS8	P62198	2 (2)
28S ribosomal protein S26, mitochondrial precursor	RT26	Q9EPJ3	3 (10)
3,2-trans-enoyl-CoA isomerase, mitochondrial precursor	D3D2	P23965	2 (5)
3-hydroxyacyl-CoA dehydrogenase type II	HCD2	O70351	8 (22)
3-hydroxyanthranilate 3,4-dioxygenase	3HAO	P46953	2 (2)
3-hydroxyisobutyrate dehydrogenase, mitochondrial precursor	3HIDH	P29266	5 (11)
3-ketoacyl-CoA thiolase, mitochondrial	THIM	P13437	3 (8)
3-mercaptopyruvate sulfurtransferase	THTM	P97532	3 (5)
40S ribosomal protein S10	RS10	P63326	2 (3)
40S ribosomal protein S11	RS11	P62282	3 (6)
40S ribosomal protein S13	RS13	P62278	4 (8)
40S ribosomal protein S14	RS14	P13471	2 (3)
40S ribosomal protein S15a	RS15A	P62246	3 (3)
40S ribosomal protein S16	RS16	P62250	7 (20)
40S ribosomal protein S17	RS17	P04644	3 (6)
40S ribosomal protein S18	RS18	P62271	3 (5)
40S ribosomal protein S19	RS19	P17074	4 (6)
40S ribosomal protein S2	RS2	P27952	7 (12)
40S ribosomal protein S20	RS20	P60868	4 (6)
40S ribosomal protein S24	RS24	P62850	2 (5)
40S ribosomal protein S25	RS25	P62853	4 (9)
40S ribosomal protein S3	RS3	P62909	7 (26)
40S ribosomal protein S4, X isoform	RS4X	P62703	4 (11)
40S ribosomal protein S6	RS6	P62755	2 (5)
40S ribosomal protein S7	RS7	P62083	2 (5)
40S ribosomal protein S8	RS8	P62243	3 (15)
40S ribosomal protein S9	RS9	P29314	9 (24)
40S ribosomal protein SA	RSSA	P38983	6 (22)
5-aminolevulinate synthase, erythroid-specific, mitochondrial precursor	HEM0	Q63147	2 (6)
5-hydroxytryptamine 2A receptor	5HT2A	P14842	2 (2)
60 kDa heat shock protein, mitochondrial precursor	CH60	P63039	18 (46)
60S acidic ribosomal protein P0	RLA0	P19945	7 (22)
60S acidic ribosomal protein P1	RLA1	P19944	2 (8)
60S acidic ribosomal protein P2	RLA2	P02401	6 (16)
60S ribosomal protein L10a	RL10A	P62907	2 (7)
60S ribosomal protein L13	RL13	P41123	5 (9)
60S ribosomal protein L13a	RL13A	P35427	2 (9)
60S ribosomal protein L14	RL14	Q63507	2 (7)
60S ribosomal protein L15	RL15	P61314	3 (9)
60S ribosomal protein L17	RL17	P24049	4 (6)
60S ribosomal protein L18	RL18	P12001	4 (16)
60S ribosomal protein L19	RL19	P84100	2 (2)
60S ribosomal protein L21	RL21	P20280	2 (3)
60S ribosomal protein L23	RL23	P62832	2 (5)
60S ribosomal protein L23a	RL23A	P62752	3 (6)
60S ribosomal protein L24	RL24	P83732	3 (8)
60S ribosomal protein L27	RL27	P61354	2 (4)
60S ribosomal protein L3	RL3	P21531	2 (6)
60S ribosomal protein L4	RL4	P50878	6 (11)
60S ribosomal protein L5	RL5	P09895	2 (4)
60S ribosomal protein L6	RL6	P21533	3 (7)

Protein Name	Gene Name	Accession Number	Unique Peptide Number (Spectra Number)
60S ribosomal protein L7	RL7	P05426	5 (16)
60S ribosomal protein L7a	RL7A	P62425	4 (19)
60S ribosomal protein L9	RL9	P17077	3 (3)
6-phosphofructokinase, liver type	K6PL	P30835	6 (7)
6-phosphofructokinase, muscle type	K6PF	P47858	3 (4)
6-phosphofructokinase, type C	K6PP	P47860	2 (4)
72 kDa inositol polyphosphate 5-phosphatase	INP5	Q9WVR1	2 (2)
78 kDa glucose-regulated protein precursor	GRP78	P06761	20 (59)